Dissecting the DNA binding landscape and gene regulatory network of p63 and p53

Konstantin Riege[1], Helene Kretzmer[2], Arne Sahm[1], Simon S. McDade[3], Steve Hoffmann[1], Martin Fischer[1,#]

[1] Computational Biology Group, Leibniz Institute on Aging – Fritz Lipmann Institute (FLI), Beutenbergstraße 11, 07745 Jena, Germany

[2] Department of Genome Regulation, Max Planck Institute for Molecular Genetics, Ihnestraße 63-73, 14195 Berlin, Germany

[3] Patrick G Johnston Centre for Cancer Research, Queen's University Belfast, 97 Lisburn Road, Belfast BT9 7AE, UK

Running title: p63 GRN vs p53 GRN

[#]To whom correspondence should be addressed. Email: Martin.Fischer@leibniz-fli.de

Abstract

The transcription factor p53 is the best-known tumor suppressor, but its sibling p63 is a master regulator of epidermis development and a key oncogenic driver in squamous cell carcinomas (SCC). Despite multiple gene expression studies becoming available, the limited overlap of reported p63-dependent genes has made it difficult to decipher the p63 gene regulatory network. Particularly, analyses of p63 response elements differed substantially among the studies. To address this intricate data situation, we provide an integrated resource that enables assessing the p63-dependent regulation of any human gene of interest. We use a novel iterative *de novo* motif search approach in conjunction with extensive ChIP-seq data to achieve a precise global distinction between p53 and p63 binding sites, recognition motifs, and potential co-factors. We integrate these data with enhancer:gene associations to predict p63 target genes and identify those that are commonly de-regulated in SCC representing candidates for prognosis and therapeutic interventions.

Keywords

p63, p53, gene regulation, DNA binding, squamous cell carcinoma

Introduction

In contrast to the tumor suppressor p53 with its extensive set of target genes controlling the cell cycle and apoptosis (Fischer, 2017; Sammons et al., 2020), its phylogenetically ancient sibling p63 (ΔNp63) governs epidermis development (Mills et al., 1999; Yang et al., 1999) and is an oncogenic driver of squamous cell carcinoma (SCC) (Campbell et al., 2018; Gatti et al., 2019) that is overexpressed or amplified in SCCs, which depend on its expression (Ramsey et al., 2013). Together with p73, p63 and p53 form the p53 transcription factor (TF) family that shares a highly conserved DNA binding domain (DBD) through which they bind to very similar DNA recognition motifs. The mechanisms that enable these sibling TFs to shape their unique gene regulatory network (GRN) leading to the different phenotypic control, however, remain poorly understood.

The *TP53* and *TP63* genes encode for two major isoform groups that are controlled by distinct promoters leading to transcripts differing in their N-terminus (Murray-Zmijewski et al., 2006). In the case of *TP53*, the longest isoform, p53α, is ubiquitously expressed while the alternative intronic promoter has little activity across virtually all tissues. Conversely, the usage of the two *TP63* promoters is highly cell type-dependent. For instance, the long isoform TAp63 is predominantly expressed in germ cells, while the smaller transcript, ΔNp63, is most copious in stratifying epithelia (Sethi et al., 2015). Similar to p53, alternative splicing leads to α, β, and γ protein isoforms that differ in their C-terminus (Murray-Zmijewski et al., 2006). While both TAp63 and ΔNp63 may bind to DNA through a specific binding domain, ΔNp63 lacks the canonical N-terminal transactivation domain (TAD) (Yang et al., 1998) and has long been thought to be a dominant-negative regulator of other p53 family members or its own isoforms (Gebel et al., 2016; Yang et al., 1998). However, ΔNp63 has also been shown to harbor alternative TADs, that endow transactivation activity (Helton et al., 2006; King et al., 2003; Yang et al., 2006). Notably, many ΔNp63 binding sites are associated with enhancer regions, where ΔNp63 has been proposed to “bookmark” genes that are expressed in stratifying epithelia (Karsli Uzunbas et al., 2019; Kouwenhoven et al., 2015a; Lin-Shiao et al., 2019; Qu et al., 2018; Somerville et al., 2018). Here, we focus on the most widely expressed isoforms p53α (hereafter p53) and ΔNp63 (hereafter p63).

The p53 TF family shares many binding sites, but all three family members have been shown to bind to substantial sets of unique target genes (Lin et al., 2009; McDade et al., 2014). Indeed, there are differences in the DBDs, e.g. regarding thermostability, hydrophobic potentials (Enthart et al., 2016), zinc-coordination (Lokshin et al., 2007), and redox sensitivity (Tichý et al., 2013). In addition, the different C-terminal domains (CTD) of p53 family members may also affect their DNA binding specificity (Sauer et al., 2008). p53 binds to a canonical 20 bp response element (RE) made of two decameric half-sites that both contain

the sequence RRRCWWGYYY (R = A/G; W= A/T; Y = C/T). p53 has also been shown to bind to decameric half-sites separated by spacers or to single half-sites (Kitayner et al., 2010; Menendez et al., 2013; Vyas et al., 2017). Results from systematic evolution of ligands by exponential enrichment (SELEX) (Ortt and Sinha, 2006; Perez et al., 2007) and high-throughput analyses of chromatin immunoprecipitation (ChIP) (Kouwenhoven et al., 2010; McDade et al., 2012; Yang et al., 2006) yielded p63 binding motifs with high similarity to the p53RE but still showed some unique characteristics. These unique characteristics identified for p63REs, however, differed substantially between the studies.

While multiple genome-wide p63 gene expression datasets became available in recent years, our understanding of the p63 GRN remains incomplete. This is in part due to the limited overlap of the p63-dependent genes identified in individual studies (Kouwenhoven et al., 2015b). Also, the frequent binding of p63 to enhancers (Kouwenhoven et al., 2015a; Lin-Shiao et al., 2019, 2018; Qu et al., 2018; Somerville et al., 2018) and the difficulty to associate such enhancers with target gene regulation adds another level of complexity to the quest of describing the GRN. To overcome these limitations, we utilize a recently developed meta-analysis approach (Fischer et al., 2016a), which helped us to dissect the GRNs of the mouse and human orthologue of p53 (Fischer, 2020, 2019). The analysis rests upon a ranking of potential p63 target genes based on the number of datasets supporting a p63-dependent regulation. In addition, we utilize the wealth of recent p63 and p53 ChIP-seq studies to establish a more precise global distinction between p53 and p63 binding sites and their underlying REs. This approach could serve as a blueprint to distinguish binding site specificities of TF siblings. Further integration of gene expression studies with the binding data and enhancer:gene associations enables us to predict high-probability direct p63 target genes.

Results

The p63 gene regulatory network

To identify genes commonly regulated by p63 across cell types and tissues, we employed a previously established meta-analysis approach, that has been helpful to infer core GRNs for human and mouse p53, the viral oncoprotein E7 and the cell cycle GRN (Fischer, 2019; Fischer et al., 2017, 2016a, 2014). From 11 genome-wide studies (Abraham et al., 2018; Bao et al., 2015; Carroll et al., 2006; Gallant-Behm et al., 2012; Karsli Uzunbas et al., 2019; Lin-Shiao et al., 2019; Saladi et al., 2017; Somerville et al., 2018; Watanabe et al., 2014; Wu et al., 2012; Zarnegar et al., 2012) (Supplementary File 1), 16 publically available gene expression datasets were integrated to generate a specific *p63 Expression Score* (Supplementary File 2). The datasets have been obtained from knockdown (n=12) or

overexpression experiments (n=4) of p63 in primary keratinocytes (n=3), the keratinocyte cell line HaCaT (n=2), the foreskin fibroblast cell line BJ (n=1), the breast epithelial cell line MCF10A (n=4), the squamous carcinoma cell lines H226 (n=2), KYSE70 (n=1), and FaDu (n=1), as well as the pancreatic ductal adenocarcinoma cell lines BxPC3 (n=1) and SUIT2 (n=1) (Figures 1A and 1B and Supplementary File 1).

To illustrate the utility of our approach, we selected 30 genes from various *p63 Expression Score* groups reflecting commonly up- and down-regulated ones (Figure 1C). We noted lower consistency across the data on p63-dependent gene regulation as compared to previous meta-analyses on human and mouse p53 (Fischer, 2019; Fischer et al., 2016a). In contrast to the recent investigations, data integrated here are based on a higher number of experiments in primary cells and a comparably lower number of replicates. Thus, the reduced consistency may also reflect the higher variance as opposed to data from more homogenous cell lines. Furthermore, p63-depleted cells are less viable, and the global decrease in mRNA levels may confound effects. Despite this, our approach identified genes that are commonly altered by p63.

We next performed gene set enrichment analysis (GSEA) for p63-dependently regulated genes using MSigDB gene sets (Subramanian et al., 2005). In agreement with the function of p63 as an essential proliferation factor (McDade et al., 2011; Senoo et al., 2007; Truong et al., 2006), epidermal development regulator (Mills et al., 1999; Yang et al., 1999), and MYC network activator (Wu et al., 2012), we find that genes commonly up-regulated by p63 significantly enrich gene sets associated with cell cycle, epidermis development, and MYC targets (Figure 2A). In line with previous reports (Mehta et al., 2018), genes down-regulated by p63 enrich gene sets connected with interferon response (Figure 2B). Corroborating the role of p63 in mammary stem cell activity (Chakrabarti et al., 2014) and SCC growth (Ramsey et al., 2013), we find that p63 up- and down-regulated genes enrich respective gene sets up- and down-regulated in mammary stem cells (Figure 2C) and across SCCs (Figure 2D). In addition to pathways that have been linked to p63 earlier, we find that p63 up-regulated genes enrich for mTORC1 signaling genes and p63 down-regulated genes enrich for gene sets associated with oxidative phosphorylation and aerobic respiration (Figure 2E).

Further, we performed TF binding enrichment analysis for p63-dependently regulated genes using Enrichr (Kuleshov et al., 2016). In agreement with its established roles, we identify cell cycle gene regulators (E2F4, E2F6, SIN3A, E2F1, FOXM1, NFYA, and NFYB (Fischer and Müller, 2017)) and the MYC/MAX TFs as being enriched among p63-upregulated genes. Consistent with previous reports, our analysis also identifies KLF4 (Sen et al., 2012) and SMAD4 (Calleja et al., 2016) as potential mediators of p63-dependent gene regulation. In addition, our analysis reveals that androgen receptor (AR), its co-factor ZMIZ1,

as well as SP1, FLI1, and NANOG are novel candidates for mediating the p63-dependent up-regulation of multiple genes. Surprisingly, our analysis identified only SOX2 as a frequent binder of genes down-regulated by p63 (Figure 3A). Consistent with the strong association of p63 up-regulated genes with the cell cycle (Figure 2A) and with cell cycle regulators (Figure 3A), we find that p63 up-regulated genes enrich DREAM (dimerization partner, RB-like, E2F, and multi-vulval class B) and E2F target genes (Figure 3B), and DREAM target genes appear to be modestly but consistently down-regulated when p63 is lost (Figure 3C). Notably, most datasets on p63-dependent gene expression were derived from cells in which p63 was overexpressed or depleted, without additional treatments. However, one dataset was derived from Nutlin-treated MCF10A cells (Karsli Uzunbas et al., 2019). MCF10A cells harbor wild-type p53 and DREAM targets are down-regulated in response to Nutlin treatment. Strikingly, depletion of p63 decreased their expression even further without affecting *CDKN1A* (p21) levels (Figure 3D), which indicates a possible cumulative effect that is independent of p53 regulatory functions.

Together, the meta-analysis approach overcomes the limitations of individual studies and identifies target genes supported by multiple datasets. The extensive and integrated resource on p63-regulated genes enables researchers to compare their results quickly and to identify the most promising targets.

p63 and p53 regulate largely distinct gene sets

Given that p63 and p53 share a significant number of binding sites and thus potential target genes, we next compared the *p63 Expression Score* to the previously established *p53 Expression Score* (Fischer et al., 2016a). In agreement with the up-regulation of cell cycle genes and DREAM targets through p63 (Figure 2A and 3) and their down-regulation through p53 (Fischer et al., 2016a, 2016b; Schade et al., 2019; Uxa et al., 2019), we noted that negative *p53 Expression Scores* tend to correlate with positive *p63 Expression Scores* (Figure 4A). Furthermore, the results indicate that p53-induced genes (positive *p53 Expression Scores*) appear to be largely unaffected by p63. Consistently, expression data for 343 target genes with strong evidence for direct up-regulation by p53 (Fischer, 2017), do not show consistent expression changes upon knockdown or induction of p63 (Figure 4B). Together, these results indicate that basal expression of the majority of p53 target genes is not affected by p63.

Common and distinct properties of p63 and p53 DNA binding

To identify shared p63 and p53 bound sites, we compared the 20 p63 ChIP-seq datasets (Supplementary File 1) to 28 p53 ChIP-seq datasets we compiled recently (Fischer, 2019). Notably, p63 and p53 data was collected from cells with strong basal p63 expression

and stimulated p53 expression, respectively. While the majority of all p53 ChIP-seq peaks occurs in only one of the experiments, more than half of the p63 peaks are present in two or more datasets (Figure 5A and B). Even though we were able to integrate substantially more p53 datasets, the number of identified p63 binding sites was still higher (Figure 5C). This indicates that p63 occupies many more binding sites as compared to p53. Importantly, when more datasets agree on p53 and p63 binding sites, these sequences are more likely to harbor a canonical p53 and p63RE, facilitating the motif discovery by tools such as HOMER (Heinz et al., 2010) and enriching *bona fide* binding sites (Figure 5D). Earlier meta-analyses employed a similar strategy (Fischer et al., 2016a; Nguyen et al., 2018; Verfaillie et al., 2016). To dissect the binding preferences of p63 and p53, we generated three distinct peak sets (Figure 5E). The 'p53+p63' set contained all binding sites with evidence in at least five p63 and five p53 ChIP-seq datasets. The 'p53 unique' (hereafter 'p53') set contained all binding sites that were supported by at least five p53 ChIP-seq datasets but not a single p63 dataset. We also generated a 'p63 unique' (hereafter 'p63') set *vice versa*.

We employed an iterative *de novo* motif search using HOMER to identify frequent binding site motifs. After each round, we removed all peaks harboring the best motif and repeated the search. We identified similar yet distinct binding motifs for the three groups (Figure 5F). Comparison of the primary 'p53+p63', 'p53', and 'p63' motifs suggests that p63 binding sites display a highly conserved C, G, C, and G at positions 4, 7, 14, and 17, respectively. The second round revealed a p53RE containing a 1bp spacer (p53 secondary motif), supporting the model that p53 can bind to spacer-containing p53REs (Vyas et al., 2017). The results further indicate that p53 can bind to a single half-site (p53 tertiary motif) and that this single half-site is more constrained at positions 5 and 6 as well as the flanking regions than half-sites in the canonical p53RE (e.g. primary p53+p63 and p53 motifs). Of note, these single half-sites may also include p53REs with spacers longer than 1 bp that are not detected separately because of their very low abundance. Sole half-sites together with spacer-containing p53REs underlie only ~5 % of p53 bound sites (Figure 6). Furthermore, p53 and p63 appear to be able to bind to three-quarter sites (secondary and quaternary p53+p63 and p63 motifs), while p63 can generally bind to a broader spectrum of sequences as compared to p53 (Figure 5F). This broader binding repertoire likely underlies p63's capacity to engage with substantially more binding sites than does p53.

It is important to note that the vast majority (~70 %) of p53 and p63 binding sites harbor full-length p53 and p63REs (Figure 6 and 7, Supplementary File 3). There is a good correlation between p53 and p63 binding site occupation, and most sites commonly bound by p53 are also frequently bound by p63 (Figure 5-figure supplement 1). However, p63 binds many sites that are not bound by p53 (Figure 5E and Figure 5-figure supplement 2). More importantly, p53 binding is strongly constrained to canonical p53RE (Figure 5-figure

supplement 1C-D and 2A-C). In contrast, p63 binding appears not to benefit from a more canonical p63RE (Figure 5-figure supplement 1E-F and 2D-F). These data suggest that sequence-specific binding is particularly important to recruit p53, while p63 only requires minimal sequence identity and could require additional co-factors to bind and ultimately regulate its target genes.

Therefore, we also searched for potential cooperating TFs that may be co-enriched at p53 and p63 binding sites. Consistent with earlier analyses (Verfaillie et al., 2016), no additional motif was substantially enriched in the vicinity of 'p53' or 'p53+p63' binding sites. Consistent with the co-enrichment of AP-1 and p63 at enhancers (Lin-Shiao et al., 2018), we found that unique p63 binding sites were consistently enriched for AP-1 (bZIP) in addition to bHLH motifs (Figure 5-figure supplement 3). Using the CistromeDB toolkit (R. Zheng et al., 2019), we identified TFs that significantly enrich for binding to the 'p53+p63', 'p53', and 'p63' sites. As expected, the analysis identified the p53 family members p53, p63, and p73 as best hits for the common sites, but only p53 and p73 for the unique p53 and only p63 and p73 for the unique p63 peak sets (Figure 5-figure supplement 4). In agreement with earlier studies, the analysis identified p300 (Katoh et al., 2019), MAF (Lopez-Pajares et al., 2015), SOX2 (Watanabe et al., 2014), BANF1 (also known as BAF) (Bao et al., 2015), and KMT2D (Lin-Shiao et al., 2018) as potential co-binders of p63; as well as TRIM28 (Doyle et al., 2010), BRD4 (Stewart et al., 2013), p300 (Lill et al., 1997), ZBTB33 (KAISO) (Koh et al., 2014), CDK9 (Claudio et al., 2006), and HEXIM1 (Lew et al., 2012) as potential co-binders of p53. Moreover, our analysis identified potential co-binders that to our knowledge have not been identified before, such as KDM1A, PRMT1, and GRHL2 for p63 and BRD9, ZNF131, and C17orf49 for p53. Importantly, these new potential co-binders appear to be unique to either p63 or p53, suggesting that they may contribute to shaping the DNA binding landscapes that are specific to p63 and p53 (Figure 5-figure supplement 4).

Identification of direct p63 target genes

Given that p63 regulates many target genes through enhancers (Kouwenhoven et al., 2015a; Lin-Shiao et al., 2019, 2018; Qu et al., 2018; Somerville et al., 2018), straight forward integration of differential gene regulation data and p63 binding data based on proximity binding to a gene's TSS is unlikely to capture all direct p63 target genes. To resolve this issue, we integrated the p63 binding data and the *p63 Expression Score* based on enhancer:gene association information (Fishilevich et al., 2017) in addition to proximity binding to TSSs to predict direct p63 target genes. Given the large number of p63 binding sites identified (Figure 5C and 5E) and the high variance in p63-dependent gene regulation (Figure 1B), we employed conservative thresholds to identify high-probability target genes of p63. We only used p63 binding sites supported by at least half of the datasets (≥10) that are

linked through TSS proximity (within 5 kb) or double-elite enhancer:gene associations (Fishilevich et al., 2017) to genes with a |*p63 Expression Score*| ≥ 8 (Table 1 and Figure 7-figure supplement 1). Of note, many genes are associated with proximal and enhancer p63 binding, because many proximal promoters are also identified as double-elite enhancers in the database. The 180 (138 up-regulated and 42 down-regulated) genes that passed our conservative filtering contain many genes that are known direct p63 targets, such as *RAB38* (Barton et al., 2010), *S100A2* (Kirschner et al., 2008; Lapi et al., 2006), *HAS3* (Compagnone et al., 2017), *IRF6* (Thomason et al., 2010), *PTHLH* (Somerville et al., 2018), *GPX2* (Yan and Chen, 2006), *JAG1* (Sasaki et al., 2002), *MMP14* (Lodillinsky et al., 2016), *NRG1* (Forster et al., 2014), and *PLAC8* (Gallant-Behm et al., 2012). The identification of these well-established p63 target genes indicates the ability of our approach to identify *bona fide* candidates. Importantly, the integration of enhancer:gene associations enabled the identification of genes that are likely regulated by p63 through enhancers, such as *IL1B*, *MREG*, *MYO5A*, *RRP12*, *SNCA*, *AK4*, and *EHD4* (Table 1 and Figure 7-figure supplement 1).

Table 1. High-probability direct p63 target genes. Genes identified as significantly up- or down-regulated in at least the half of all datasets (|p63 Expression Score| ≥ 8) that are linked to p63 binding sites supported by at least half of all datasets (≥ 10) through binding within 5 kb from their TSS or through double-elite enhancer-gene associations (Fishilevich et al., 2017). Using these thresholds we identified 138 and 42 high-probability candidates as directly up- and down-regulated by p63, respectively. Gene names marked in bold are also up- or down-regulated across SCCs (Campbell et al., 2018).

Gene Symbol	*p63 Expression Score*	p63 binding within 5kb from TSS	p63 binding linked through enhancer	Gene Symbol	*p63 Expression Score*	p63 binding within 5kb from TSS	p63 binding linked through enhancer
DUSP6	14	yes	yes	*FSCN1*	8	yes	yes
RAB38	14	yes	yes	*GINS3*	8	yes	no
GSDME	13	yes	yes	*GM2A*	8	yes	yes
LAD1	13	yes	yes	***HMGA2***	8	yes	yes
S100A2	13	yes	yes	*HSPA4L*	8	yes	yes
TMEM40	13	yes	yes	*JAG1*	8	yes	yes
FGFBP1	12	yes	yes	*KCTD12*	8	yes	no
HAS3	12	yes	no	*KIAA0930*	8	yes	yes
NECTIN1	12	yes	yes	*KIF14*	8	no	yes
TCOF1	12	yes	yes	*KIRREL1*	8	no	yes
DUSP7	11	yes	yes	*LIG1*	8	yes	yes
IL1B	11	no	yes	***LPAR3***	8	yes	yes
MREG	11	no	yes	*LRRFIP2*	8	no	yes
PA2G4	11	yes	no	*MALT1*	8	no	yes

RGS20	11	yes	no	*MAST4*	8	no	yes
SDC1	11	no	yes	*MCM3*	8	no	yes
SFN	11	yes	yes	***MMP14***	8	yes	yes
STK17A	11	yes	yes	*MMRN2*	8	yes	no
VSNL1	11	yes	yes	*NOM1*	8	yes	no
ARHGAP25	10	yes	yes	*NRCAM*	8	yes	yes
CDCA4	10	yes	yes	*NRG1*	8	no	yes
DUSP11	10	yes	no	*OAS3*	8	yes	yes
FAT2	10	yes	no	*PPFIBP1*	8	yes	yes
FERMT1	10	yes	yes	*PROCR*	8	yes	no
IL4R	10	yes	yes	*QSOX2*	8	yes	yes
INPP1	10	yes	yes	*RAD51C*	8	yes	yes
IRF6	10	no	yes	***RASSF6***	8	no	yes
ITGA6	10	no	yes	*RFX7*	8	yes	no
KIZ	10	yes	no	*SH3PXD2A*	8	no	yes
MAPKBP1	10	no	yes	*SLC1A5*	8	yes	yes
MYO10	10	yes	yes	*SLC2A9*	8	yes	yes
MYO19	10	yes	yes	*SLC37A2*	8	yes	no
ORC1	10	no	yes	*SMAD5*	8	yes	no
PAK1	10	yes	no	*SPATS2*	8	no	yes
PTHLH	10	yes	yes	*SSRP1*	8	no	yes
SMTN	10	yes	no	*TGFB1*	8	yes	yes
WDFY2	10	yes	no	*TMEM237*	8	yes	no
XDH	10	yes	yes	*TOMM34*	8	yes	no
ARHGDIB	9	yes	yes	***TRIM7***	8	yes	yes
AURKB	9	yes	no	*TRIP13*	8	yes	no
BTBD11	9	yes	no	*TSPAN5*	8	yes	no
C6orf106	9	yes	no	*TSR1*	8	no	yes
CARD10	9	yes	yes	*TYMS*	8	yes	yes
CHAF1A	9	no	yes	*UCK2*	8	yes	yes
CSTA	9	yes	no	*UTP4*	8	no	yes
CYP27B1	9	yes	no	*YAP1*	8	yes	no
FEZ1	9	yes	yes	*YES1*	8	yes	yes
GNA15	9	yes	no	*ZFP36L2*	8	no	yes
GPX2	9	yes	no	*APH1B*	-8	no	yes
GSTP1	9	yes	no	*BIRC3*	-8	yes	yes
HRAS	9	yes	yes	*C9orf3*	-8	yes	yes
IFI16	9	yes	yes	*CHST3*	-8	no	yes
KREMEN1	9	yes	yes	*CPQ*	-8	no	yes
LDLR	9	yes	no	*DUSP8*	-8	yes	no
MAPK6	9	yes	yes	*EPCAM*	-8	no	yes
MYO5A	9	no	yes	*ERBB2*	-8	no	yes
NCAPH2	9	yes	no	*FBN1*	-8	no	yes
NDE1	9	yes	yes	*ITFG1*	-8	yes	no
NDST1	9	yes	yes	*LLGL2*	-8	yes	yes
NIPAL4	9	yes	yes	*NCSTN*	-8	no	yes
PPIF	9	no	yes	*OPN3*	-8	no	yes

PPP4R4	9	yes	no	***PBX1***	-8	yes	yes
PTTG1	9	yes	yes	*PDXK*	-8	no	yes
RAPGEF5	9	yes	yes	*PLAC8*	-8	yes	yes
RNASE7	9	yes	yes	*S100A4*	-8	no	yes
RRP12	9	no	yes	***SPOCK1***	-8	no	yes
SERPINB13	9	yes	no	*TNS3*	-8	no	yes
SNCA	9	no	yes	*ARL6IP5*	-9	no	yes
STX6	9	yes	no	***COBL***	-9	no	yes
AK4	8	no	yes	*CUEDC1*	-9	yes	yes
ARHGAP23	8	yes	yes	*GSN*	-9	yes	no
ASCC3	8	yes	yes	*PDGFC*	-9	yes	yes
BRCA1	8	yes	no	*PGPEP1*	-9	no	yes
BTBD10	8	yes	yes	*PLXNB2*	-9	yes	yes
CCNK	8	yes	no	*PXDN*	-9	no	yes
CCT4	8	yes	no	*RALGPS1*	-9	yes	yes
CD44	8	yes	yes	*ROR1*	-9	yes	no
CDC42SE1	8	yes	no	*SLC16A5*	-9	yes	yes
CDCA7	8	yes	no	*TM4SF1*	-9	yes	yes
COL17A1	8	yes	no	*ALDH3B1*	-10	yes	yes
CRKL	8	yes	yes	***CYP1B1***	-10	no	yes
DRAP1	8	yes	yes	*HHAT*	-10	yes	yes
EHD4	8	no	yes	*MEGF8*	-10	no	yes
ERCC6L	8	no	yes	*PTGES*	-10	yes	no
ESRP1	8	no	yes	*PTTG1IP*	-10	no	yes
FABP5	8	yes	no	*RPS27L*	-10	yes	yes
FANCI	8	yes	yes	*SECTM1*	-10	yes	yes
FLOT2	8	yes	no	*SLC22A5*	-10	yes	no
FOSL1	8	yes	yes	*TNFSF15*	-10	yes	yes
FRMD4B	8	yes	no	*SRD5A3*	-11	yes	no

A p63/SCC 28-gene set correlates with HNSC patient survival

Out of the 180 high-probability p63 target genes 32 (28 up- and 4 down-regulated) are also identified as being commonly up- or down-regulated in SCCs compared to non-SCC cancers (Campbell et al., 2018) (Table 1). Importantly, several of the genes commonly up-regulated by p63 as well as in SCC have been identified to promote SCC growth or invasion, such as *LAD1* (Abe et al., 2019), *TMEM40* (Zhang et al., 2019), *FGFBP1* (Czubayko et al., 1997), *IL1B* (Lee et al., 2015), *FAT2* (Dang et al., 2016), *FOSL1* (Usui et al., 2012), *LPAR3* (Brusevold et al., 2014), *MMP14* (Pang et al., 2016), and *RASSF6* (L. Zheng et al., 2019). Therefore, we asked whether the set of 28 up-regulated direct p63 targets correlates with patient survival. To this end, we employed data of head and neck SCC (HNSC) patients from The Cancer Genome Atlas (TCGA). Notably, it is known that this cancer type frequently harbors amplified *TP63* (Lawrence et al., 2015). We find that expression levels of our gene set indeed correlate significantly negatively with HNSC patient survival (COX likelihood ratio

test p=0.032). To determine whether expression levels of the set have an influence on the survival of HNSC patients, we subdivided the samples according to the average expression levels into four equally sized groups (low, low-med, med-high, high). While the sample group with low expression had the most favorable prognosis, the null hypothesis could not be rejected in the direct comparison with patients with high average expression levels (p=0.090; Figure 8A). However, upon contrasting the low-expression group with all remaining samples, a significant improvement of survival was detected (p=0.024; Figure 8B). Expression of the 28-gene set correlated positively with p63 expression when p63 expression was rather low (FPKM <20), but showed a saturation and no further correlation when p63 expression was high (FPKM >20; Figure 8C, 8D, and Figure 8-figure supplement 1). This indicates that p63 levels influence the 28-gene set in a switch-like manner where a saturation of p63-dependent activation is quickly reached in HNSC cells. Together, these findings indicate that the genes commonly up-regulated by p63 and in SCC influence the prognosis of HNSC patients. Taken together, this finding calls for a more detailed assessment of ubiquitous p63/SCC genes as biomarkers in the future.

Discussion

Although p63 (ΔNp63) is known as master regulator in epidermis development and more recently emerged as a key oncogenic factor in SCC, a comprehensive assessment of the GRN commonly controlled by p63 and its comparison to the GRN commonly controlled by the closely related tumor suppressor p53 has been missing. An increasing number of available high-throughput datasets enabled us to generate ranked lists of p63-regulated genes and p63 bound DNA sites that together reveal high-probability direct p63 target genes regulated by p63 across cells of multiple origins. Because p63 target genes, very much like p53 target genes (Fischer, 2020, 2019), differ substantially between mouse and human (Sethi et al., 2017), many p63 target genes initially described in mouse could not be confirmed to be p63-regulated in this study using human data. Given that p63 binding sites are frequently associated with enhancer regions and enhancer identity, we have integrated enhancer:gene associations to identify target genes that are regulated by p63 through direct binding to associated enhancers. This approach enabled the identification of novel direct target genes that are missed by standard analyses that employ only TSS proximity (Table 1 and Figure 7-figure supplement 1).

Given the similarity between their DBDs, it has been a long-standing question how p53 and p63 bind to distinct sites in the genome and how these sites differ from another. Several studies found differences in the biochemical properties of p53 and p63 that could affect their DNA binding specificity (Enthart et al., 2016; Lokshin et al., 2007; Sauer et al.,

2008; Tichý et al., 2013). Various studies aimed to identify the precise p63 recognition motif and its difference from the p53RE using either SELEX (Ortt and Sinha, 2006; Perez et al., 2007) or ChIP-seq data (Kouwenhoven et al., 2010; McDade et al., 2014; Yang et al., 2006), yet these studies reported different features as being unique for p63 compared to p53 DNA recognition. By combining multiple ChIP-seq datasets we have contributed here to better distinguish between sites commonly bound by p53 and p63 across cell types and sites that are unique to p53 or p63 (Figure 5E). Most importantly, our results could explain why a substantial fraction of DNA sites is occupied exclusively by p53 or p63. While most sites bound by p53 are also commonly occupied by p63 (Figure 5E and Figure 5-figure supplement 1A), single half-sites and half-sites separated by spacers underlie many sites that are only bound by p53 (Figure 5F and 6), supporting earlier findings whereby p53 can be recruited through spacer-containing motifs (Vyas et al., 2017). However, while spacers reportedly have been identified in fifty percent of 200 analyzed p53REs (Vyas et al., 2017), our genome-wide quantification of motifs underlying 7705 high confidence p53 peaks based on an unbiased motif search using HOMER revealed that only 1.1 to 5.1% of the p53 peaks contain p53REs with 1 bp spacers or half sites that are possibly separated by longer spacers (Figure 6). Mechanistically, our results imply that relying on the CWWG core motif and the flanking regions may enable p53 to bind to those sites. In contrast, the two CNNG core motifs that underlie p63, but not p53REs, offer an explanation why a substantial fraction of DNA sites is bound exclusively by p63 (Figure 5F and 7), supporting one of the models established earlier (McDade et al., 2014). Notably, p63's ability to bind to a greater variety of recognition motifs likely underlies the markedly greater number of p63 compared to p53 binding sites in the genome. In addition, our motif search indicates that factors bound to AP-1 (bZIP) and bHLH motifs may specifically support p63 binding (Figure 5-figure supplement 3), and transcription factor enrichment analysis identified the bZIP TF MAF, the TF GRHL2, the chromatin remodeler BANF1, the histone methyltransferase PRMT1, and the ZNF750/KDM1A/KLF4 complex, which was previously shown to operate downstream of p63 (Boxer et al., 2014), as potential co-binders that could help to facilitate p63 binding to certain genomic loci (Figure 5-figure supplement 4). Considering its pioneer role, p63 could *vice versa* enable the binding of these TFs to the respective loci. Given that p63 and p73 form stable heterotetramers (Gebel et al., 2016), p73 may possess binding specificities that are highly similar to those identified for p63. Our results indicate that our approach could serve as a blueprint to distinguish DNA recognition motifs, binding sites, co-factors, and target genes of TF siblings more precisely. Our iterative *de novo* search algorithm enabled the identification of spacer-containing p53REs, indicating that our approach uncovers second-tier TF binding motifs invisible to standard approaches. Moreover, the results provide insights to the p63 DNA binding repertoire in unprecedented depth (Figure 5F).

Consistent with results from an earlier genome-wide study (Yang et al., 2006), our findings imply that p63 is more frequently involved in a direct up-regulation as opposed to a direct down-regulation of target genes (Figure 3A and Figure 7-figure supplement 1). Mechanistically, p63 has been shown to up-regulate target genes through its alternative TAD located at the N-terminus while the C-terminus is important for down-regulation (Helton et al., 2006). Exogenous expression of different isoforms of p53 family members and their antagonistic effects on target gene promoters in luciferase reporter assays suggested a model whereby p63 exhibits a dominant negative effect on other p53 family members (Mundt et al., 2010; Westfall et al., 2003; Yang et al., 1998). Inconsistent with its reputation as dominant negative regulator of p53, however, genome-wide studies showed that the groups of p63-regulated genes and p53-regulated genes show only very little overlap (Gallant-Behm et al., 2012). A recent analysis of DNA sites bound and of genes regulated by p53 and p63 revealed that p63 is more likely to support than to inhibit p53 activity (Karsli Uzunbas et al., 2019). Our analysis further supports the notion that p63 does not commonly interfere with target gene up-regulation by p53 but that except for cell cycle genes they regulate largely distinct gene sets (Figure 4).

We identify several candidate TFs that may operate downstream of p63 and that may serve as transitional nodes in the p63 GRN. In addition to known mediators of p63-dependent gene regulation, such as MYC and KLF4, we identify AR and its co-factor ZMIZ1, SP1, FLI1, and NANOG as novel candidate nodes in the p63 GRN (Figure 3A). In agreement with the tumor suppressor role of p53 and the oncogenic role of p63, we find that cell cycle genes are antagonistically regulated by p53 and p63 (Figure 2A and 4A). On the one hand, cell cycle genes are well-known to be down-regulated by p53 indirectly through the cyclin-dependent kinase inhibitor p21 and the cell cycle repressor complexes DREAM and RB-E2F (Fischer et al., 2016a, 2016b; Schade et al., 2019; Uxa et al., 2019). On the other hand, cell cycle genes are down-regulated upon loss of p63 and this p63-dependent regulation reportedly occurs through regulating p21 signaling and the DREAM component p130 (McDade et al., 2011; Truong et al., 2006). In addition to indirect effects, we also predicted multiple cell cycle genes as direct p63 targets (Table 1). Consequently, a loss of p63 may substantially contribute to the effect of p53 in reducing cell cycle gene expression (Figure 3D). In addition of p63's role in driving the expression of some cell cycle genes, the entire set of cell cycle genes may be subsequently up-regulated indirectly through p63's pro-proliferative targets. While the up-regulation of cell cycle genes occurs in most cancers (Whitfield et al., 2006), we find that p63 additionally regulates genes that are specifically altered across SCCs (Figure 2D). These results underscore the critical role of p63 and its target genes in determining the transcriptional profile of SCC. An example of a p63 target in SCC is NRG1, which can be inhibited to block SCC proliferation and tumor growth (Hegde et

al., 2019). The resource of genes commonly regulated by p63 provided here may help to identify targets that can be exploited therapeutically. We provided a showcase example, where expression levels of the 28 p63 target genes that are commonly up-regulated by p63 and in SCC (Table 1) correlate significantly with poorer survival of HNSC patients (Figure 8). Thus, this 28-gene set may contain particularly promising candidates for therapeutic interventions and for the use as biomarkers.

Methods

Re-analysis and integration of publicly available gene expression profiling datasets

We re-analyzed publicly available p63-dependent gene expression profiling datasets. As a first quality requirement, we only included datasets for re-analysis that contained at least two biological replicates for the treatment as well as for the control condition. All microarray datasets were available at a pre-processed stage at the Gene Expression Omnibus (GEO) and we re-analyzed these datasets with GEO2R to obtain fold expression changes and Benjamini Hochberg-corrected p-values (Clough and Barrett, 2016). Gene identifiers were mapped to Ensembl Gene IDs using the Ensembl annotation data (Cunningham et al., 2019). All RNA-seq datasets have been retrieved through GEO from the Sequence Read Archive (SRA) (Leinonen et al., 2011). We employed our RNA-seq analysis pipeline to obtain fold expression changes and p-values adjusted for multiple testing. Briefly, we utilized Trimmomatic (Bolger et al., 2014) v0.39 (5nt sliding window approach, mean quality cutoff 22) for read quality trimming according to inspections made from FastQC (https://www.bioinformatics.babraham.ac.uk/projects/fastqc/) v0.11.8 reports. Clipping was performed using Cutadapt v2.3 (Martin, 2011). Potential sequencing errors were detected and corrected using Rcorrector v1.0.3.1 (Song and Florea, 2015). Ribosomal RNA (rRNA) transcripts were artificially depleted by read alignment against rRNA databases through SortMeRNA v2.1 (Kopylova et al., 2012). The preprocessed data was aligned to the reference genome hg38, retrieved along with its gene annotation from Ensembl v.92 (Cunningham et al., 2019). For read alignment, we used the splice-aware mapping software segemehl (Hoffmann et al., 2014, 2009) v0.3.4 with adjusted accuracy (95%). Mappings were filtered by Samtools v1.9 (Li et al., 2009) for uniqueness and properly aligned mate pairs. Read quantification was performed on exon level using featureCounts v1.6.5 (Liao et al., 2014), parametrized according to the strand specificity inferred through RSeQC v3.0.0 (Wang et al., 2012). Differential gene expression and its statistical significance was identified using DESeq2 v1.20.0 (Love et al., 2014). Information on the samples that were compared for each dataset is included in Supplementary File 1. Given that all RNA-seq data was derived from PolyA-enriched samples, we only included Ensembl transcript types ‘protein_coding’, ‘antisense’, ‘lincRNA’ and ‘TEC’ in our analysis. Common thresholds for adj. p-value ≤ 0.05 were applied.

Generation of the p63 Expression Score

For 19,156 genes covered by at least three datasets including a minimum of one RNA-seq dataset, a *p63 Expression Score* was calculated as the number of datasets that find the gene to be significantly up-regulated minus the number of datasets that find the gene

to be significantly down-regulated in dependence on p63. This meta-analysis resulted in 27 *p63 Expression Score* gene groups because no gene was identified as up-regulated in all 16 or 15 datasets or down-regulated in all 16, 15, 14 or 13 datasets.

Enrichment analyses

Gene set enrichment analysis (GSEA) was performed using GSEA (http://software.broadinstitute.org/gsea/) with 'H', 'C2', and 'C6' gene sets from MSigDB v7.0 (Subramanian et al., 2005) and custom panSCC gene sets derived from Table S1C in Campbell *et al.* (Campbell et al., 2018). GSEA was performed on a pre-ranked list of genes that were ranked primarily by *p63 Expression Score* and secondarily by median $\log_2$(fold-change) to obtain unique ranks.

Enrichment of transcription factor binding to genes with high (≥ 8) or low (≤ -8) *p63 Expression Score* was identified using the results section 'ENCODE and ChEA Consensus TFs from ChIP-X' from Enrichr (Kuleshov et al., 2016).

Integration of publicly available p63 and p53 binding data

Peak datasets from p63 ChIP-seq experiments were retrieved from CistromeDB (R. Zheng et al., 2019) (Supplementary File 1). When replicate experiments were available, all peaks were used that have been identified in at least two replicates. A similar collection of p53 peak datasets has been described previously (Fischer, 2019). To intersect multiple peak files Bedtools 'multiinter' was used and to identify overlapping and non-overlapping peaks Bedtools 'intersect' was employed (Quinlan and Hall, 2010).

Motif search

Known p53 and p63REs were identified using the 'known motifs' in HOMER v4.10 with default options and *-size given* (Heinz et al., 2010). *De novo* motif discovery was performed with options *-size given -len 10,15,20,25 -mis 5 -S 10*.

Identification of potential co-factors

We used the CistromeDB toolkit (R. Zheng et al., 2019) to identify TFs that display ChIP-seq peaksets that are significantly similar to our 'unique p53', 'unique p63', and 'p53+p63' peaksets.

Survival and expression correlation analysis

For the 28-gene set, single-sample enrichment scores were derived from FPKM normalized gene expression values of 546 HNSC patient samples. To this end, we utilized the official GenePattern single sample gene set enrichment analysis (ssGSEA) codebase

v10.0.3 (https://github.com/GSEA-MSigDB/ssGSEA-gpmodule). A sample score represents the coordinately up- or down-regulated expression of all genes within one set as its signature (Barbie et al., 2009). Kaplan-Meier plots and correlation analyses were performed on TCGA time to event and event occurrence information using the R survival package v3.2-3. Following the TCGA standard for HNSC (Lawrence et al., 2015), survival analyses were right-censored at 60 months (1800 days) to avoid non-cancer-related events. The Cox proportional hazards model was used to investigate the association of patient survival time and the combined expression levels of the 28-gene set. Subsequently, we subdivided the expression scores into four equally sized categorical groups (high, med-high, med-low, low). The rates of occurrence of events over time were compared between these groups using the fitted COX PH model.

We retrieved read quantification data 'HTSeq - Counts' from 546 samples of the TCGA project HNSC utilizing the R package TCGAbiolinks v2.18.0 (Colaprico et al., 2016). Per sample, all read counts of the 28-gene set were merged into an artificially created metagene. Subsequently, we calculated normalized expression values per gene as fragments per kilobase million, where the length of a gene corresponds to the lengths of its exons assigned to either the canonical transcript (CCDS) or the longest transcript according to hg38 Ensembl annotation v92. *TP63* FPKM values were plotted against the meta-gene FPKM value or the ssGSEA derived gene set scores (see above).

Funding

This work was supported through the German Research Foundation (DFG) [FI 1993/2-1 to MF] and the German Federal Ministry for Education and Research (BMBF) [031L016D to SH]. Funding for open access charge: Leibniz Institute on Aging - Fritz Lipmann Institute (FLI). The FLI is a member of the Leibniz Association and is financially supported by the Federal Government of Germany and the State of Thuringia.

Conflicts of interest

The authors declare no conflict of interest.

Reference List

Abe DT, Yamazaki DM, Maruyama DS, Ajioka PY. 2019. Ladinin-1 is involved in cell motility and proliferation of oral squamous cell carcinoma cells. *Oral Surg Oral Med Oral Pathol Oral Radiol* **128**:e81–e82. doi:10.1016/j.oooo.2019.02.205

Abraham CG, Ludwig MP, Andrysik Z, Pandey A, Joshi M, Galbraith MD, Sullivan KD, Espinosa JM. 2018. ΔNp63α Suppresses TGFB2 Expression and RHOA Activity to Drive Cell Proliferation in Squamous Cell Carcinomas. *Cell Rep* **24**:3224–3236.

536 doi:10.1016/j.celrep.2018.08.058
537 Bao X, Rubin AJ, Qu K, Zhang J, Giresi PG, Chang HY, Khavari PA. 2015. A novel ATAC-
538 seq approach reveals lineage-specific reinforcement of the open chromatin landscape
539 via cooperation between BAF and p63. *Genome Biol* **16**:284. doi:10.1186/s13059-015-
540 0840-9
541 Barbie DA, Tamayo P, Boehm JS, Kim SY, Moody SE, Dunn IF, Schinzel AC, Sandy P,
542 Meylan E, Scholl C, Fröhling S, Chan EM, Sos ML, Michel K, Mermel C, Silver SJ, Weir
543 BA, Reiling JH, Sheng Q, Gupta PB, Wadlow RC, Le H, Hoersch S, Wittner BS,
544 Ramaswamy S, Livingston DM, Sabatini DM, Meyerson M, Thomas RK, Lander ES,
545 Mesirov JP, Root DE, Gilliland DG, Jacks T, Hahn WC. 2009. Systematic RNA
546 interference reveals that oncogenic KRAS-driven cancers require TBK1. *Nature*
547 **462**:108–112. doi:10.1038/nature08460
548 Barton CE, Johnson KN, Mays DM, Boehnke K, Shyr Y, Boukamp P, Pietenpol JA. 2010.
549 Novel p63 target genes involved in paracrine signaling and keratinocyte differentiation.
550 *Cell Death Dis* **1**:e74. doi:10.1038/cddis.2010.49
551 Bolger AM, Lohse M, Usadel B. 2014. Trimmomatic: a flexible trimmer for Illumina sequence
552 data. *Bioinformatics* **30**:2114–2120. doi:10.1093/bioinformatics/btu170
553 Boxer LD, Barajas B, Tao S, Zhang J, Khavari PA. 2014. Znf750 interacts with KLF4 and
554 RCOR1, KDM1A, And CTBP1/2 chromatin regulators to repress epidermal progenitor
555 genes and induce differentiation genes. *Genes Dev* **28**:2013–2026.
556 doi:10.1101/gad.246579.114
557 Brusevold IJ, Tveteraas IH, Aasrum M, Ødegård J, Sandnes DL, Christoffersen T. 2014.
558 Role of LPAR3, PKC and EGFR in LPA-induced cell migration in oral squamous
559 carcinoma cells. *BMC Cancer* **14**. doi:10.1186/1471-2407-14-432
560 Calleja LR, Jacques C, Lamoureux F, Baud'Huin M, Gabriel MT, Quillard T, Sahay D, Perrot
561 P, Amiaud J, Charrier C, Brion R, Lecanda F, Verrecchia F, Heymann D, Ellisen LW,
562 Ory B. 2016. ΔNp63α silences a miRNA program to aberrantly initiate a wound-healing
563 program that promotes TGFβ-induced metastasis. *Cancer Res* **76**:3236–3251.
564 doi:10.1158/0008-5472.CAN-15-2317
565 Campbell JD, Yau C, Bowlby R, Liu Y, Brennan K, Fan H, Taylor AM, Wang C, Walter V,
566 Akbani R, Byers LA, Creighton CJ, Coarfa C, Shih J, Cherniack AD, Gevaert O,
567 Prunello M, Shen H, Anur P, Chen J, Cheng H, Hayes DN, Bullman S, Pedamallu CS,
568 Ojesina AI, Sadeghi S, Mungall KL, Robertson AG, Benz C, Schultz A, Kanchi RS, Gay
569 CM, Hegde A, Diao L, Wang Jing, Ma W, Sumazin P, Chiu H-S, Chen T-W, Gunaratne
570 P, Donehower L, Rader JS, Zuna R, Al-Ahmadie H, Lazar AJ, Flores ER, Tsai KY, Zhou
571 JH, Rustgi AK, Drill E, Shen R, Wong CK, Stuart JM, Laird PW, Hoadley KA, Weinstein
572 JN, Peto M, Pickering CR, Chen Z, Van Waes C, Caesar-Johnson SJ, Demchok JA,
573 Felau I, Kasapi M, Ferguson ML, Hutter CM, Sofia HJ, Tarnuzzer R, Wang Z, Yang L,
574 Zenklusen JC, Zhang J (Julia), Chudamani S, Liu J, Lolla L, Naresh R, Pihl T, Sun Q,
575 Wan Y, Wu Y, Cho J, DeFreitas T, Frazer S, Gehlenborg N, Getz G, Heiman DI, Kim J,
576 Lawrence MS, Lin P, Meier S, Noble MS, Saksena G, Voet D, Zhang Hailei, Bernard B,
577 Chambwe N, Dhankani V, Knijnenburg T, Kramer R, Leinonen K, Liu Y, Miller M,
578 Reynolds S, Shmulevich I, Thorsson V, Zhang W, Akbani R, Broom BM, Hegde AM, Ju
579 Z, Kanchi RS, Korkut A, Li J, Liang H, Ling S, Liu W, Lu Y, Mills GB, Ng K-S, Rao A,
580 Ryan M, Wang Jing, Weinstein JN, Zhang J, Abeshouse A, Armenia J, Chakravarty D,
581 Chatila WK, de Bruijn I, Gao J, Gross BE, Heins ZJ, Kundra R, La K, Ladanyi M, Luna
582 A, Nissan MG, Ochoa A, Phillips SM, Reznik E, Sanchez-Vega F, Sander C, Schultz N,
583 Sheridan R, Sumer SO, Sun Y, Taylor BS, Wang Jioajiao, Zhang Hongxin, Anur P, Peto
584 M, Spellman P, Benz C, Stuart JM, Wong CK, Yau C, Hayes DN, Parker JS, Wilkerson
585 MD, Ally A, Balasundaram M, Bowlby R, Brooks D, Carlsen R, Chuah E, Dhalla N, Holt
586 R, Jones SJM, Kasaian K, Lee D, Ma Y, Marra MA, Mayo M, Moore RA, Mungall AJ,
587 Mungall K, Robertson AG, Sadeghi S, Schein JE, Sipahimalani P, Tam A, Thiessen N,
588 Tse K, Wong T, Berger AC, Beroukhim R, Cherniack AD, Cibulskis C, Gabriel SB, Gao
589 GF, Ha G, Meyerson M, Schumacher SE, Shih J, Kucherlapati MH, Kucherlapati RS,
590 Baylin S, Cope L, Danilova L, Bootwalla MS, Lai PH, Maglinte DT, Van Den Berg DJ,
591 Weisenberger DJ, Auman JT, Balu S, Bodenheimer T, Fan C, Hoadley KA, Hoyle AP,

Jefferys SR, Jones CD, Meng S, Mieczkowski PA, Mose LE, Perou AH, Perou CM, Roach J, Shi Y, Simons J V., Skelly T, Soloway MG, Tan D, Veluvolu U, Fan H, Hinoue T, Laird PW, Shen H, Zhou W, Bellair M, Chang K, Covington K, Creighton CJ, Dinh H, Doddapaneni H, Donehower LA, Drummond J, Gibbs RA, Glenn R, Hale W, Han Y, Hu J, Korchina V, Lee S, Lewis L, Li W, Liu X, Morgan M, Morton D, Muzny D, Santibanez J, Sheth M, Shinbrot E, Wang L, Wang M, Wheeler DA, Xi L, Zhao F, Hess J, Appelbaum EL, Bailey M, Cordes MG, Ding L, Fronick CC, Fulton LA, Fulton RS, Kandoth C, Mardis ER, McLellan MD, Miller CA, Schmidt HK, Wilson RK, Crain D, Curley E, Gardner J, Lau K, Mallery D, Morris S, Paulauskis J, Penny R, Shelton C, Shelton T, Sherman M, Thompson E, Yena P, Bowen J, Gastier-Foster JM, Gerken M, Leraas KM, Lichtenberg TM, Ramirez NC, Wise L, Zmuda E, Corcoran N, Costello T, Hovens C, Carvalho AL, de Carvalho AC, Fregnani JH, Longatto-Filho A, Reis RM, Scapulatempo-Neto C, Silveira HCS, Vidal DO, Burnette A, Eschbacher J, Hermes B, Noss A, Singh R, Anderson ML, Castro PD, Ittmann M, Huntsman D, Kohl B, Le X, Thorp R, Andry C, Duffy ER, Lyadov V, Paklina O, Setdikova G, Shabunin A, Tavobilov M, McPherson C, Warnick R, Berkowitz R, Cramer D, Feltmate C, Horowitz N, Kibel A, Muto M, Raut CP, Malykh A, Barnholtz-Sloan JS, Barrett W, Devine K, Fulop J, Ostrom QT, Shimmel K, Wolinsky Y, Sloan AE, De Rose A, Giuliante F, Goodman M, Karlan BY, Hagedorn CH, Eckman J, Harr J, Myers J, Tucker K, Zach LA, Deyarmin B, Hu H, Kvecher L, Larson C, Mural RJ, Somiari S, Vicha A, Zelinka T, Bennett J, Iacocca M, Rabeno B, Swanson P, Latour M, Lacombe L, Têtu B, Bergeron A, McGraw M, Staugaitis SM, Chabot J, Hibshoosh H, Sepulveda A, Su T, Wang T, Potapova O, Voronina O, Desjardins L, Mariani O, Roman-Roman S, Sastre X, Stern M-H, Cheng F, Signoretti S, Berchuck A, Bigner D, Lipp E, Marks J, McCall S, McLendon R, Secord A, Sharp A, Behera M, Brat DJ, Chen A, Delman K, Force S, Khuri F, Magliocca K, Maithel S, Olson JJ, Owonikoko T, Pickens A, Ramalingam S, Shin DM, Sica G, Van Meir EG, Zhang Hongzheng, Eijckenboom W, Gillis A, Korpershoek E, Looijenga L, Oosterhuis W, Stoop H, van Kessel KE, Zwarthoff EC, Calatozzolo C, Cuppini L, Cuzzubbo S, DiMeco F, Finocchiaro G, Mattei L, Perin A, Pollo B, Chen C, Houck J, Lohavanichbutr P, Hartmann A, Stoehr C, Stoehr R, Taubert H, Wach S, Wullich B, Kycler W, Murawa D, Wiznerowicz M, Chung K, Edenfield WJ, Martin J, Baudin E, Bubley G, Bueno R, De Rienzo A, Richards WG, Kalkanis S, Mikkelsen T, Noushmehr H, Scarpace L, Girard N, Aymerich M, Campo E, Giné E, Guillermo AL, Van Bang N, Hanh PT, Phu BD, Tang Y, Colman H, Evason K, Dottino PR, Martignetti JA, Gabra H, Juhl H, Akeredolu T, Stepa S, Hoon D, Ahn K, Kang KJ, Beuschlein F, Breggia A, Birrer M, Bell D, Borad M, Bryce AH, Castle E, Chandan V, Cheville J, Copland JA, Farnell M, Flotte T, Giama N, Ho T, Kendrick M, Kocher J-P, Kopp K, Moser C, Nagorney D, O'Brien D, O'Neill BP, Patel T, Petersen G, Que F, Rivera M, Roberts L, Smallridge R, Smyrk T, Stanton M, Thompson RH, Torbenson M, Yang JD, Zhang L, Brimo F, Ajani JA, Gonzalez AMA, Behrens C, Bondaruk J, Broaddus R, Czerniak B, Esmaeli B, Fujimoto J, Gershenwald J, Guo C, Lazar AJ, Logothetis C, Meric-Bernstam F, Moran C, Ramondetta L, Rice D, Sood A, Tamboli P, Thompson T, Troncoso P, Tsao A, Wistuba I, Carter C, Haydu L, Hersey P, Jakrot V, Kakavand H, Kefford R, Lee K, Long G, Mann G, Quinn M, Saw R, Scolyer R, Shannon K, Spillane A, Stretch O, Synott M, Thompson J, Wilmott J, Al-Ahmadie H, Chan TA, Ghossein R, Gopalan A, Levine DA, Reuter V, Singer S, Singh B, Tien NV, Broudy T, Mirsaidi C, Nair P, Drwiega P, Miller J, Smith J, Zaren H, Park J-W, Hung NP, Kebebew E, Linehan WM, Metwalli AR, Pacak K, Pinto PA, Schiffman M, Schmidt LS, Vocke CD, Wentzensen N, Worrell R, Yang H, Moncrieff M, Goparaju C, Melamed J, Pass H, Botnariuc N, Caraman I, Cernat M, Chemencedji I, Clipca A, Doruc S, Gorincioi G, Mura S, Pirtac M, Stancul I, Tcaciuc D, Albert M, Alexopoulou I, Arnaout A, Bartlett J, Engel J, Gilbert S, Parfitt J, Sekhon H, Thomas G, Rassl DM, Rintoul RC, Bifulco C, Tamakawa R, Urba W, Hayward N, Timmers H, Antenucci A, Facciolo F, Grazi G, Marino M, Merola R, de Krijger R, Gimenez-Roqueplo A-P, Piché A, Chevalier S, McKercher G, Birsoy K, Barnett G, Brewer C, Farver C, Naska T, Pennell NA, Raymond D, Schilero C, Smolenski K, Williams F, Morrison C, Borgia JA, Liptay MJ, Pool M, Seder CW, Junker K, Omberg L, Dinkin M, Manikhas G, Alvaro D, Bragazzi MC,

Cardinale V, Carpino G, Gaudio E, Chesla D, Cottingham S, Dubina M, Moiseenko F, Dhanasekaran R, Becker K-F, Janssen K-P, Slotta-Huspenina J, Abdel-Rahman MH, Aziz D, Bell S, Cebulla CM, Davis A, Duell R, Elder JB, Hilty J, Kumar B, Lang J, Lehman NL, Mandt R, Nguyen P, Pilarski R, Rai K, Schoenfield L, Senecal K, Wakely P, Hansen P, Lechan R, Powers J, Tischler A, Grizzle WE, Sexton KC, Kastl A, Henderson J, Porten S, Waldmann J, Fassnacht M, Asa SL, Schadendorf D, Couce M, Graefen M, Huland H, Sauter G, Schlomm T, Simon R, Tennstedt P, Olabode O, Nelson M, Bathe O, Carroll PR, Chan JM, Disaia P, Glenn P, Kelley RK, Landen CN, Phillips J, Prados M, Simko J, Smith-McCune K, VandenBerg S, Roggin K, Fehrenbach A, Kendler A, Sifri S, Steele R, Jimeno A, Carey F, Forgie I, Mannelli M, Carney M, Hernandez B, Campos B, Herold-Mende C, Jungk C, Unterberg A, von Deimling A, Bossler A, Galbraith J, Jacobus L, Knudson M, Knutson T, Ma D, Milhem M, Sigmund R, Godwin AK, Madan R, Rosenthal HG, Adebamowo C, Adebamowo SN, Boussioutas A, Beer D, Giordano T, Mes-Masson A-M, Saad F, Bocklage T, Landrum L, Mannel R, Moore K, Moxley K, Postier R, Walker J, Zuna R, Feldman M, Valdivieso F, Dhir R, Luketich J, Pinero EMM, Quintero-Aguilo M, Carlotti CG, Dos Santos JS, Kemp R, Sankarankuty A, Tirapelli D, Catto J, Agnew K, Swisher E, Creaney J, Robinson B, Shelley CS, Godwin EM, Kendall S, Shipman C, Bradford C, Carey T, Haddad A, Moyer J, Peterson L, Prince M, Rozek L, Wolf G, Bowman R, Fong KM, Yang I, Korst R, Rathmell WK, Fantacone-Campbell JL, Hooke JA, Kovatich AJ, Shriver CD, DiPersio J, Drake B, Govindan R, Heath S, Ley T, Van Tine B, Westervelt P, Rubin MA, Lee J Il, Aredes ND, Mariamidze A. 2018. Genomic, Pathway Network, and Immunologic Features Distinguishing Squamous Carcinomas. *Cell Rep* **23**:194-212.e6. doi:10.1016/j.celrep.2018.03.063

Carroll DK, Carroll JS, Leong C-O, Cheng F, Brown M, Mills AA, Brugge JS, Ellisen LW. 2006. p63 regulates an adhesion programme and cell survival in epithelial cells. *Nat Cell Biol* **8**:551–61. doi:10.1038/ncb1420

Chakrabarti R, Wei Y, Hwang J, Hang X, Andres Blanco M, Choudhury A, Tiede B, Romano RA, Decoste C, Mercatali L, Ibrahim T, Amadori D, Kannan N, Eaves CJ, Sinha S, Kang Y. 2014. Δnp63 promotes stem cell activity in mammary gland development and basal-like breast cancer by enhancing Fzd7 expression and Wnt signalling. *Nat Cell Biol* **16**:1004–1015. doi:10.1038/ncb3040

Claudio PP, Cui J, Ghafouri M, Mariano C, White MK, Safak M, Sheffield JB, Giordano A, Khalili K, Amini S, Sawaya BE. 2006. Cdk9 phosphorylates p53 on serine 392 independently of CKII. *J Cell Physiol* **208**:602–612. doi:10.1002/jcp.20698

Clough E, Barrett T. 2016. The Gene Expression Omnibus Database. *Methods Mol Biol* **1418**:93–110. doi:10.1007/978-1-4939-3578-9_5

Colaprico A, Silva TC, Olsen C, Garofano L, Cava C, Garolini D, Sabedot TS, Malta TM, Pagnotta SM, Castiglioni I, Ceccarelli M, Bontempi G, Noushmehr H. 2016. TCGAbiolinks: An R/Bioconductor package for integrative analysis of TCGA data. *Nucleic Acids Res* **44**:e71. doi:10.1093/nar/gkv1507

Compagnone M, Gatti V, Presutti D, Ruberti G, Fierro C, Markert EK, Vousden KH, Zhou H, Mauriello A, Anemone L, Bongiorno-Borbone L, Melino G, Peschiaroli A. 2017. ΔNp63-mediated regulation of hyaluronic acid metabolism and signaling supports HNSCC tumorigenesis. *Proc Natl Acad Sci* **114**:13254–13259. doi:10.1073/pnas.1711777114

Cunningham F, Achuthan P, Akanni W, Allen J, Amode MR, Armean IM, Bennett R, Bhai J, Billis K, Boddu S, Cummins C, Davidson C, Dodiya KJ, Gall A, Girón CG, Gil L, Grego T, Haggerty L, Haskell E, Hourlier T, Izuogu OG, Janacek SH, Juettemann T, Kay M, Laird MR, Lavidas I, Liu Z, Loveland JE, Marugán JC, Maurel T, McMahon AC, Moore B, Morales J, Mudge JM, Nuhn M, Ogeh D, Parker A, Parton A, Patricio M, Abdul Salam AI, Schmitt BM, Schuilenburg H, Sheppard D, Sparrow H, Stapleton E, Szuba M, Taylor K, Threadgold G, Thormann A, Vullo A, Walts B, Winterbottom A, Zadissa A, Chakiachvili M, Frankish A, Hunt SE, Kostadima M, Langridge N, Martin FJ, Muffato M, Perry E, Ruffier M, Staines DM, Trevanion SJ, Aken BL, Yates AD, Zerbino DR, Flicek P. 2019. Ensembl 2019. *Nucleic Acids Res* **47**:D745–D751. doi:10.1093/nar/gky1113

Czubayko F, Liaudet-Coopman EDE, Aigner A, Tuveson AT, Berchem GJ, Wellstein A. 1997. A secreted FGF-binding protein can serve as the angiogenic switch in human

cancer. *Nat Med* **3**:1137–1140. doi:10.1038/nm1097-1137
Dang TT, Westcott JM, Maine EA, Kanchwala M, Xing C, Pearson GW. 2016. ΔNp63α induces the expression of FAT2 and Slug to promote tumor invasion. *Oncotarget* **7**:28592–611. doi:10.18632/oncotarget.8696
Doyle JM, Gao J, Wang J, Yang M, Potts PR. 2010. MAGE-RING protein complexes comprise a family of E3 ubiquitin ligases. *Mol Cell* **39**:963–974. doi:10.1016/j.molcel.2010.08.029
Enthart A, Klein C, Dehner A, Coles M, Gemmecker G, Kessler H, Hagn F. 2016. Solution structure and binding specificity of the p63 DNA binding domain. *Sci Rep* **6**:26707. doi:10.1038/srep26707
Fischer M. 2020. Mice Are Not Humans: The Case of p53. *Trends in cancer*. doi:10.1016/j.trecan.2020.08.007
Fischer M. 2019. Conservation and divergence of the p53 gene regulatory network between mice and humans. *Oncogene* **38**:4095–4109. doi:10.1038/s41388-019-0706-9
Fischer M. 2017. Census and evaluation of p53 target genes. *Oncogene* **36**:3943–3956. doi:10.1038/onc.2016.502
Fischer M, Grossmann P, Padi M, DeCaprio JA. 2016a. Integration of TP53, DREAM, MMB-FOXM1 and RB-E2F target gene analyses identifies cell cycle gene regulatory networks. *Nucleic Acids Res* **44**:6070–6086. doi:10.1093/nar/gkw523
Fischer M, Müller GA. 2017. Cell cycle transcription control: DREAM/MuvB and RB-E2F complexes. *Crit Rev Biochem Mol Biol* **52**:638–662. doi:10.1080/10409238.2017.1360836
Fischer M, Quaas M, Steiner L, Engeland K. 2016b. The p53-p21-DREAM-CDE/CHR pathway regulates G2/M cell cycle genes. *Nucleic Acids Res* **44**:164–174. doi:10.1093/nar/gkv927
Fischer M, Steiner L, Engeland K. 2014. The transcription factor p53: Not a repressor, solely an activator. *Cell Cycle* **13**:3037–3058. doi:10.4161/15384101.2014.949083
Fischer M, Uxa S, Stanko C, Magin TM, Engeland K. 2017. Human papilloma virus E7 oncoprotein abrogates the p53-p21-DREAM pathway. *Sci Rep* **7**:2603. doi:10.1038/s41598-017-02831-9
Fishilevich S, Nudel R, Rappaport N, Hadar R, Plaschkes I, Iny Stein T, Rosen N, Kohn A, Twik M, Safran M, Lancet D, Cohen D. 2017. GeneHancer: genome-wide integration of enhancers and target genes in GeneCards. *Database (Oxford)* **2017**. doi:10.1093/database/bax028
Forster N, Saladi SV, van Bragt M, Sfondouris ME, Jones FE, Li Z, Ellisen LW. 2014. Basal Cell Signaling by p63 Controls Luminal Progenitor Function and Lactation via NRG1. *Dev Cell* **28**:147–160. doi:10.1016/j.devcel.2013.11.019
Gallant-Behm CL, Ramsey MR, Bensard CL, Nojek I, Tran J, Liu M, Ellisen LW, Espinosa JM. 2012. ΔNp63α represses anti-proliferative genes via H2A.Z deposition. *Genes Dev* **26**:2325–36. doi:10.1101/gad.198069.112
Gatti V, Fierro C, Annicchiarico-Petruzzelli M, Melino G, Peschiaroli A. 2019. ΔNp63 in squamous cell carcinoma: defining the oncogenic routes affecting epigenetic landscape and tumour microenvironment. *Mol Oncol* **13**:1878–0261.12473. doi:10.1002/1878-0261.12473
Gebel J, Luh LM, Coutandin D, Osterburg C, Löhr F, Schäfer B, Frombach A-S, Sumyk M, Buchner L, Krojer T, Salah E, Mathea S, Güntert P, Knapp S, Dötsch V. 2016. Mechanism of TAp73 inhibition by ΔNp63 and structural basis of p63/p73 hetero-tetramerization. *Cell Death Differ* **23**:1930–1940. doi:10.1038/cdd.2016.83
Hegde G V, de la Cruz C, Giltnane JM, Crocker L, Venkatanarayan A, Schaefer G, Dunlap D, Hoeck JD, Piskol R, Gnad F, Modrusan Z, de Sauvage FJ, Siebel CW, Jackson EL. 2019. NRG1 is a critical regulator of differentiation in TP63-driven squamous cell carcinoma. *Elife* **8**. doi:10.7554/elife.46551
Heinz S, Benner C, Spann N, Bertolino E, Lin YC, Laslo P, Cheng JX, Murre C, Singh H, Glass CK. 2010. Simple combinations of lineage-determining transcription factors prime cis-regulatory elements required for macrophage and B cell identities. *Mol Cell* **38**:576–89. doi:10.1016/j.molcel.2010.05.004

760 Helton ES, Zhu J, Chen X. 2006. The unique NH2-terminally deleted (DeltaN) residues, the
761 PXXP motif, and the PPXY motif are required for the transcriptional activity of the
762 DeltaN variant of p63. *J Biol Chem* **281**:2533–42. doi:10.1074/jbc.M507964200
763 Hoffmann S, Otto C, Doose G, Tanzer A, Langenberger D, Christ S, Kunz M, Holdt LM,
764 Teupser D, Hackermüller J, Stadler PF. 2014. A multi-split mapping algorithm for
765 circular RNA, splicing, trans-splicing and fusion detection. *Genome Biol* **15**:R34.
766 doi:10.1186/gb-2014-15-2-r34
767 Hoffmann S, Otto C, Kurtz S, Sharma CM, Khaitovich P, Vogel J, Stadler PF, Hackermüller
768 J. 2009. Fast Mapping of Short Sequences with Mismatches, Insertions and Deletions
769 Using Index Structures. *PLoS Comput Biol* **5**:e1000502.
770 doi:10.1371/journal.pcbi.1000502
771 Karsli Uzunbas G, Ahmed F, Sammons MA. 2019. Control of p53-dependent transcription
772 and enhancer activity by the p53 family member p63. *J Biol Chem* **294**:10720–10736.
773 doi:10.1074/jbc.RA119.007965
774 Katoh I, Maehata Y, Moriishi K, Hata RI, Kurata S ichi. 2019. C-terminal α Domain of p63
775 Binds to p300 to Coactivate β-Catenin. *Neoplasia (United States)* **21**:494–503.
776 doi:10.1016/j.neo.2019.03.010
777 King KE, Ponnamperuma RM, Yamashita T, Tokino T, Lee LA, Young MF, Weinberg WC.
778 2003. deltaNp63alpha functions as both a positive and a negative transcriptional
779 regulator and blocks in vitro differentiation of murine keratinocytes. *Oncogene* **22**:3635–
780 44. doi:10.1038/sj.onc.1206536
781 Kirschner RD, Sänger K, Müller GA, Engeland K. 2008. Transcriptional activation of the
782 tumor suppressor and differentiation gene S100A2 by a novel p63-binding site. *Nucleic*
783 *Acids Res* **36**:2969–2980. doi:10.1093/nar/gkn132
784 Kitayner M, Rozenberg H, Rohs R, Suad O, Rabinovich D, Honig B, Shakked Z. 2010.
785 Diversity in DNA recognition by p53 revealed by crystal structures with Hoogsteen base
786 pairs. *Nat Struct Mol Biol* **17**:423–429. doi:10.1038/nsmb.1800
787 Koh DI, Han D, Ryu H, Choi W Il, Jeon BN, Kim MK, Kim Y, Kim JY, Parry L, Clarke AR,
788 Reynolds AB, Hur MW. 2014. KAISO, a critical regulator of p53-mediated transcription
789 of CDKN1A and apoptotic genes. *Proc Natl Acad Sci U S A* **111**:15078–15083.
790 doi:10.1073/pnas.1318780111
791 Kopylova E, Noé L, Touzet H. 2012. SortMeRNA: Fast and accurate filtering of ribosomal
792 RNAs in metatranscriptomic data. *Bioinformatics* **28**:3211–3217.
793 doi:10.1093/bioinformatics/bts611
794 Kouwenhoven EN, Oti M, Niehues H, van Heeringen SJ, Schalkwijk J, Stunnenberg HG,
795 Bokhoven H, Zhou H. 2015a. Transcription factor p63 bookmarks and regulates
796 dynamic enhancers during epidermal differentiation. *EMBO Rep* **16**:863–878.
797 doi:10.15252/embr.201439941
798 Kouwenhoven EN, van Bokhoven H, Zhou H. 2015b. Gene regulatory mechanisms
799 orchestrated by p63 in epithelial development and related disorders. *Biochim Biophys*
800 *Acta - Gene Regul Mech* **1849**:590–600. doi:10.1016/j.bbagrm.2015.03.003
801 Kouwenhoven EN, van Heeringen SJ, Tena JJ, Oti M, Dutilh BE, Alonso ME, de la Calle-
802 Mustienes E, Smeenk L, Rinne T, Parsaulian L, Bolat E, Jurgelenaite R, Huynen MA,
803 Hoischen A, Veltman JA, Brunner HG, Roscioli T, Oates E, Wilson M, Manzanares M,
804 Gómez-Skarmeta JL, Stunnenberg HG, Lohrum M, van Bokhoven H, Zhou H. 2010.
805 Genome-Wide Profiling of p63 DNA–Binding Sites Identifies an Element that Regulates
806 Gene Expression during Limb Development in the 7q21 SHFM1 Locus. *PLoS Genet*
807 **6**:e1001065. doi:10.1371/journal.pgen.1001065
808 Kuleshov M V., Jones MR, Rouillard AD, Fernandez NF, Duan Q, Wang Z, Koplev S, Jenkins
809 SL, Jagodnik KM, Lachmann A, McDermott MG, Monteiro CD, Gundersen GW,
810 Ma'ayan A. 2016. Enrichr: a comprehensive gene set enrichment analysis web server
811 2016 update. *Nucleic Acids Res* **44**:W90–W97. doi:10.1093/nar/gkw377
812 Lapi E, Iovino A, Fontemaggi G, Soliera AR, Iacovelli S, Sacchi A, Rechavi G, Givol D,
813 Blandino G, Strano S. 2006. S100A2 gene is a direct transcriptional target of p53
814 homologues during keratinocyte differentiation. *Oncogene* **25**:3628–37.
815 doi:10.1038/sj.onc.1209401

Lawrence MS, Sougnez C, Lichtenstein L, Cibulskis K, Lander E, Gabriel SB, Getz G, Ally A, Balasundaram M, Birol I, Bowlby R, Brooks D, Butterfield YSN, Carlsen R, Cheng D, Chu A, Dhalla N, Guin R, Holt RA, Jones SJM, Lee D, Li HI, Marra MA, Mayo M, Moore RA, Mungall AJ, Robertson AG, Schein JE, Sipahimalani P, Tam A, Thiessen N, Wong T, Protopopov A, Santoso N, Lee S, Parfenov M, Zhang Jianhua, Mahadeshwar HS, Tang J, Ren X, Seth S, Haseley P, Zeng D, Yang Lixing, Xu AW, Song X, Pantazi A, Bristow CA, Hadjipanayis A, Seidman J, Chin L, Park PJ, Kucherlapati R, Akbani R, Casasent T, Liu W, Lu Y, Mills G, Motter T, Weinstein J, Diao L, Wang J, Hong Fan Y, Liu J, Wang K, Auman JT, Balu S, Bodenheimer T, Buda E, Hayes DN, Hoadley KA, Hoyle AP, Jefferys SR, Jones CD, Kimes PK, Liu Yufeng, Marron JS, Meng S, Mieczkowski PA, Mose LE, Parker JS, Perou CM, Prins JF, Roach J, Shi Y, Simons J V., Singh D, Soloway MG, Tan D, Veluvolu U, Walter V, Waring S, Wilkerson MD, Wu J, Zhao N, Cherniack AD, Hammerman PS, Tward AD, Pedamallu CS, Saksena G, Jung J, Ojesina AI, Carter SL, Zack TI, Schumacher SE, Beroukhim R, Freeman SS, Meyerson M, Cho J, Noble MS, DiCara D, Zhang H, Heiman DI, Gehlenborg N, Voet D, Lin P, Frazer S, Stojanov P, Liu Yingchun, Zou L, Kim J, Muzny D, Doddapaneni HV, Kovar C, Reid J, Morton D, Han Y, Hale W, Chao H, Chang K, Drummond JA, Gibbs RA, Kakkar N, Wheeler D, Xi L, Ciriello G, Ladanyi M, Lee W, Ramirez R, Sander C, Shen R, Sinha R, Weinhold N, Taylor BS, Aksoy BA, Dresdner G, Gao J, Gross B, Jacobsen A, Reva B, Schultz N, Sumer SO, Sun Y, Chan TA, Morris LG, Stuart J, Benz S, Ng S, Benz C, Yau C, Baylin SB, Cope L, Danilova L, Herman JG, Bootwalla M, Maglinte DT, Laird PW, Triche T, Weisenberger DJ, Van Den Berg DJ, Agrawal N, Bishop J, Boutros PC, Bruce JP, Byers LA, Califano J, Carey TE, Chen Z, Cheng H, Chiosea SI, Cohen E, Diergaarde B, Egloff AM, El-Naggar AK, Ferris RL, Frederick MJ, Grandis JR, Guo Y, Haddad RI, Harris T, Hui ABY, Lee JJ, Lippman SM, Liu FF, McHugh JB, Myers J, Ng PKS, Perez-Ordonez B, Pickering CR, Prystowsky M, Romkes M, Saleh AD, Sartor MA, Seethala R, Seiwert TY, Si H, Van Waes C, Waggott DM, Wiznerowicz M, Yarbrough WG, Zhang Jiexin, Zuo Z, Burnett K, Crain D, Gardner J, Lau K, Mallery D, Morris S, Paulauskis J, Penny R, Shelton C, Shelton T, Sherman M, Yena P, Black AD, Bowen J, Frick J, Gastier-Foster JM, Harper HA, Leraas K, Lichtenberg TM, Ramirez NC, Wise L, Zmuda E, Baboud J, Jensen MA, Kahn AB, Pihl TD, Pot DA, Srinivasan D, Walton JS, Wan Y, Burton RA, Davidsen T, Demchok JA, Eley G, Ferguson ML, Mills Shaw KR, Ozenberger BA, Sheth M, Sofia HJ, Tarnuzzer R, Wang Z, Yang Liming, Zenklusen JC, Saller C, Tarvin K, Chen C, Bollag R, Weinberger P, Golusiński W, Golusiński P, Ibbs M, Korski K, Mackiewicz A, Suchorska W, Szybiak B, Curley E, Beard C, Mitchell C, Sandusky G, Ahn J, Khan Z, Irish J, Waldron J, William WN, Egea S, Gomez-Fernandez C, Herbert L, Bradford CR, Chepeha DB, Haddad AS, Jones TR, Komarck CM, Malakh M, Moyer JS, Nguyen A, Peterson LA, Prince ME, Rozek LS, Taylor EG, Walline HM, Wolf GT, Boice L, Chera BS, Funkhouser WK, Gulley ML, Hackman TG, Hayward MC, Huang M, Rathmell WK, Salazar AH, Shockley WW, Shores CG, Thorne L, Weissler MC, Wrenn S, Zanation AM, Brown BT, Pham M. 2015. Comprehensive genomic characterization of head and neck squamous cell carcinomas. *Nature* **517**:576–582. doi:10.1038/nature14129

Lee CH, Chang JSM, Syu SH, Wong TS, Chan JYW, Tang YC, Yang ZP, Yang WC, Chen CT, Lu SC, Tang PH, Yang TC, Chu PY, Hsiao JR, Liu KJ. 2015. IL-1β promotes malignant transformation and tumor aggressiveness in oral cancer. *J Cell Physiol* **230**:875–884. doi:10.1002/jcp.24816

Leinonen R, Sugawara H, Shumway M, International Nucleotide Sequence Database Collaboration. 2011. The sequence read archive. *Nucleic Acids Res* **39**:D19-21. doi:10.1093/nar/gkq1019

Lew QJ, Chia YL, Chu KL, Lam YT, Gurumurthy M, Xu S, Lam KP, Cheong N, Chao SH. 2012. Identification of HEXIM1 as a positive regulator of p53. *J Biol Chem* **287**:36443–36454. doi:10.1074/jbc.M112.374157

Li H, Handsaker B, Wysoker A, Fennell T, Ruan J, Homer N, Marth G, Abecasis G, Durbin R. 2009. The Sequence Alignment/Map format and SAMtools. *Bioinformatics* **25**:2078–2079. doi:10.1093/bioinformatics/btp352

Liao Y, Smyth GK, Shi W. 2014. FeatureCounts: An efficient general purpose program for assigning sequence reads to genomic features. *Bioinformatics* **30**:923–930. doi:10.1093/bioinformatics/btt656

Lill NL, Grossman SR, Ginsberg D, DeCaprio J, Livingston DM. 1997. Binding and modulation of p53 by p300/CBP coactivators. *Nature* **387**:823–7. doi:10.1038/42981

Lin-Shiao E, Lan Y, Coradin M, Anderson A, Donahue G, Simpson CL, Sen P, Saffie R, Busino L, Garcia BA, Berger SL, Capell BC. 2018. KMT2D regulates p63 target enhancers to coordinate epithelial homeostasis. *Genes Dev* **32**:181–193. doi:10.1101/gad.306241.117

Lin-Shiao E, Lan Y, Welzenbach J, Alexander KA, Zhang Z, Knapp M, Mangold E, Sammons M, Ludwig KU, Berger SL. 2019. p63 establishes epithelial enhancers at critical craniofacial development genes. *Sci Adv* **5**:eaaw0946. doi:10.1126/sciadv.aaw0946

Lin Y-L, Sengupta S, Gurdziel K, Bell GW, Jacks T, Flores ER. 2009. p63 and p73 transcriptionally regulate genes involved in DNA repair. *PLoS Genet* **5**:e1000680. doi:10.1371/journal.pgen.1000680

Lodillinsky C, Infante E, Guichard A, Chaligné R, Fuhrmann L, Cyrta J, Irondelle M, Lagoutte E, Vacher S, Bonsang-Kitzis H, Glukhova M, Reyal F, Bièche I, Vincent-Salomon A, Chavrier P. 2016. p63/MT1-MMP axis is required for in situ to invasive transition in basal-like breast cancer. *Oncogene* **35**:344–357. doi:10.1038/onc.2015.87

Lokshin M, Li Y, Gaiddon C, Prives C. 2007. p53 and p73 display common and distinct requirements for sequence specific binding to DNA. *Nucleic Acids Res* **35**:340–52. doi:10.1093/nar/gkl1047

Lopez-Pajares V, Qu K, Zhang J, Webster DE, Barajas BC, Siprashvili Z, Zarnegar BJ, Boxer LD, Rios EJ, Tao S, Kretz M, Khavari PA. 2015. A LncRNA-MAF:MAFB transcription factor network regulates epidermal differentiation. *Dev Cell* **32**:693–706. doi:10.1016/j.devcel.2015.01.028

Love MI, Huber W, Anders S. 2014. Moderated estimation of fold change and dispersion for RNA-seq data with DESeq2. *Genome Biol* **15**:550. doi:10.1186/s13059-014-0550-8

Martin M. 2011. Cutadapt removes adapter sequences from high-throughput sequencing reads. *EMBnet.journal* **17**:10. doi:10.14806/ej.17.1.200

McDade SS, Henry AE, Pivato GP, Kozarewa I, Mitsopoulos C, Fenwick K, Assiotis I, Hakas J, Zvelebil M, Orr N, Lord CJ, Patel D, Ashworth A, McCance DJ. 2012. Genome-wide analysis of p63 binding sites identifies AP-2 factors as co-regulators of epidermal differentiation. *Nucleic Acids Res* **40**:7190–7206. doi:10.1093/nar/gks389

McDade SS, Patel D, McCance DJ. 2011. p63 maintains keratinocyte proliferative capacity through regulation of Skp2-p130 levels. *J Cell Sci* **124**:1635–1643. doi:10.1242/jcs.084723

McDade SS, Patel D, Moran M, Campbell J, Fenwick K, Kozarewa I, Orr NJ, Lord CJ, Ashworth AA, McCance DJ. 2014. Genome-wide characterization reveals complex interplay between TP53 and TP63 in response to genotoxic stress. *Nucleic Acids Res* **42**:6270–6285. doi:10.1093/nar/gku299

Mehta SY, Morten BC, Antony J, Henderson L, Lasham A, Campbell H, Cunliffe H, Horsfield JA, Reddel RR, Avery-Kiejda KA, Print CG, Braithwaite AW. 2018. Regulation of the interferon-gamma (IFN-γ) pathway by p63 and Δ133p53 isoform in different breast cancer subtypes. *Oncotarget* **9**:29146–29161. doi:10.18632/oncotarget.25635

Menendez D, Nguyen TA, Freudenberg JM, Mathew VJ, Anderson CW, Jothi R, Resnick MA. 2013. Diverse stresses dramatically alter genome-wide p53 binding and transactivation landscape in human cancer cells. *Nucleic Acids Res* **41**:7286–7301. doi:10.1093/nar/gkt504

Mills AA, Zheng B, Wang XJ, Vogel H, Roop DR, Bradley A. 1999. P63 Is a P53 Homologue Required for Limb and Epidermal Morphogenesis. *Nature* **398**:708–713. doi:10.1038/19531

Mundt HM, Stremmel W, Melino G, Krammer PH, Schilling T, Müller M. 2010. Dominant negative (ΔN) p63α induces drug resistance in hepatocellular carcinoma by interference with apoptosis signaling pathways. *Biochem Biophys Res Commun* **396**:335–341. doi:10.1016/j.bbrc.2010.04.093

928 Murray-Zmijewski F, Lane DP, Bourdon J-C. 2006. P53/P63/P73 Isoforms: an Orchestra of
929 Isoforms To Harmonise Cell Differentiation and Response To Stress. *Cell Death Differ*
930 **13**:962–972. doi:10.1038/sj.cdd.4401914
931 Nguyen T-AT, Grimm SA, Bushel PR, Li J, Li Y, Bennett BD, Lavender CA, Ward JM, Fargo
932 DC, Anderson CW, Li L, Resnick MA, Menendez D. 2018. Revealing a human p53
933 universe. *Nucleic Acids Res* **46**:8153–8167. doi:10.1093/nar/gky720
934 Ortt K, Sinha S. 2006. Derivation of the consensus DNA-binding sequence for p63 reveals
935 unique requirements that are distinct from p53. *FEBS Lett* **580**:4544–4550.
936 doi:10.1016/j.febslet.2006.07.004
937 Pang L, Li Q, Li S, He J, Cao W, Lan J, Sun B, Zou H, Wang C, Liu R, Wei C, Wei Y, Qi Y,
938 Hu J, Liang W, Zhang WJ, Wan M, Li F. 2016. Membrane type 1-matrix
939 metalloproteinase induces epithelial-to-mesenchymal transition in esophageal
940 squamous cell carcinoma: Observations from clinical and in vitro analyses. *Sci Rep* **6**.
941 doi:10.1038/srep22179
942 Perez CA, Ott J, Mays DJ, Pietenpol JA. 2007. p63 consensus DNA-binding site:
943 identification, analysis and application into a p63MH algorithm. *Oncogene* **26**:7363–
944 7370. doi:10.1038/sj.onc.1210561
945 Qu J, Tanis SEJ, Smits JPH, Kouwenhoven EN, Oti M, van den Bogaard EH, Logie C,
946 Stunnenberg HG, van Bokhoven H, Mulder KW, Zhou H. 2018. Mutant p63 Affects
947 Epidermal Cell Identity through Rewiring the Enhancer Landscape. *Cell Rep* **25**:3490-
948 3503.e4. doi:10.1016/j.celrep.2018.11.039
949 Quinlan AR, Hall IM. 2010. BEDTools: A flexible suite of utilities for comparing genomic
950 features. *Bioinformatics* **26**:841–842. doi:10.1093/bioinformatics/btq033
951 Ramsey MR, Wilson C, Ory B, Rothenberg SM, Faquin W, Mills AA, Ellisen LW. 2013.
952 FGFR2 signaling underlies p63 oncogenic function in squamous cell carcinoma. *J Clin*
953 *Invest* **123**:3525–3538. doi:10.1172/JCI68899
954 Saladi SV, Ross K, Karaayvaz M, Tata PR, Mou H, Rajagopal J, Ramaswamy S, Ellisen LW.
955 2017. ACTL6A Is Co-Amplified with p63 in Squamous Cell Carcinoma to Drive YAP
956 Activation, Regenerative Proliferation, and Poor Prognosis. *Cancer Cell* **31**:35–49.
957 doi:10.1016/j.ccell.2016.12.001
958 Sammons MA, Nguyen T-AT, McDade SS, Fischer M. 2020. Tumor suppressor p53: from
959 engaging DNA to target gene regulation. *Nucleic Acids Res* **48**:8848–8869.
960 doi:10.1093/nar/gkaa666
961 Sasaki Y, Ishida S, Morimoto I, Yamashita T, Kojima T, Kihara C, Tanaka T, Imai K,
962 Nakamura Y, Tokino T. 2002. The *p53* Family Member Genes Are Involved in the Notch
963 Signal Pathway. *J Biol Chem* **277**:719–724. doi:10.1074/jbc.M108080200
964 Sauer M, Bretz AC, Beinoraviciute-Kellner R, Beitzinger M, Burek C, Rosenwald A, Harms
965 GS, Stiewe T. 2008. C-terminal diversity within the p53 family accounts for differences
966 in DNA binding and transcriptional activity. *Nucleic Acids Res* **36**:1900–12.
967 doi:10.1093/nar/gkn044
968 Schade AE, Fischer M, DeCaprio JA. 2019. RB, p130 and p107 differentially repress G1/S
969 and G2/M genes after p53 activation. *Nucleic Acids Res* **47**:11197–11208.
970 doi:10.1093/nar/gkz961
971 Sen GL, Boxer LD, Webster DE, Bussat RT, Qu K, Zarnegar BJ, Johnston D, Siprashvili Z,
972 Khavari PA. 2012. ZNF750 Is a p63 Target Gene that Induces KLF4 to Drive Terminal
973 Epidermal Differentiation. *Dev Cell* **22**:669–677. doi:10.1016/j.devcel.2011.12.001
974 Senoo M, Pinto F, Crum CP, McKeon F. 2007. p63 Is Essential for the Proliferative Potential
975 of Stem Cells in Stratified Epithelia. *Cell* **129**:523–536. doi:10.1016/j.cell.2007.02.045
976 Sethi I, Gluck C, Zhou H, Buck MJ, Sinha S. 2017. Evolutionary re-wiring of p63 and the
977 epigenomic regulatory landscape in keratinocytes and its potential implications on
978 species-specific gene expression and phenotypes. *Nucleic Acids Res* **45**:8208–8224.
979 doi:10.1093/nar/gkx416
980 Sethi I, Romano R-A, Gluck C, Smalley K, Vojtesek B, Buck MJ, Sinha S. 2015. A global
981 analysis of the complex landscape of isoforms and regulatory networks of p63 in human
982 cells and tissues. *BMC Genomics* **16**:584. doi:10.1186/s12864-015-1793-9
983 Somerville TDD, Xu Y, Miyabayashi K, Tiriac H, Cleary CR, Maia-Silva D, Milazzo JP,

Tuveson DA, Vakoc CR. 2018. TP63-Mediated Enhancer Reprogramming Drives the Squamous Subtype of Pancreatic Ductal Adenocarcinoma. *Cell Rep* **25**:1741-1755.e7. doi:10.1016/j.celrep.2018.10.051

Song L, Florea L. 2015. Rcorrector: efficient and accurate error correction for Illumina RNA-seq reads. *Gigascience* **4**:48. doi:10.1186/s13742-015-0089-y

Stewart HJS, Horne GA, Bastow S, Chevassut TJT. 2013. BRD4 associates with p53 in DNMT3A-mutated leukemia cells and is implicated in apoptosis by the bromodomain inhibitor JQ1. *Cancer Med* **2**:826–835. doi:10.1002/cam4.146

Subramanian A, Tamayo P, Mootha VK, Mukherjee S, Ebert BL, Gillette MA, Paulovich A, Pomeroy SL, Golub TR, Lander ES, Mesirov JP. 2005. Gene set enrichment analysis: A knowledge-based approach for interpreting genome-wide expression profiles. *Proc Natl Acad Sci* **102**:15545–15550. doi:10.1073/pnas.0506580102

Thomason HA, Zhou H, Kouwenhoven EN, Dotto G-P, Restivo G, Nguyen B-C, Little H, Dixon MJ, van Bokhoven H, Dixon J. 2010. Cooperation between the transcription factors p63 and IRF6 is essential to prevent cleft palate in mice. *J Clin Invest* **120**:1561–9. doi:10.1172/JCI40266

Tichý V, Navrátilová L, Adámik M, Fojta M, Brázdová M. 2013. Redox state of p63 and p73 core domains regulates sequence-specific DNA binding. *Biochem Biophys Res Commun* **433**:445–449. doi:10.1016/j.bbrc.2013.02.097

Truong AB, Kretz M, Ridky TW, Kimmel R, Khavari PA. 2006. p63 regulates proliferation and differentiation of developmentally mature keratinocytes. *Genes Dev* **20**:3185–3197. doi:10.1101/gad.1463206

Usui A, Hoshino I, Akutsu Y, Sakata H, Nishimori T, Murakami K, Kano M, Shuto K, Matsubara H. 2012. The molecular role of Fra-1 and its prognostic significance in human esophageal squamous cell carcinoma. *Cancer* **118**:3387–3396. doi:10.1002/cncr.26652

Uxa S, Bernhart SH, Mages CFS, Fischer M, Kohler R, Hoffmann S, Stadler PF, Engeland K, Müller GA. 2019. DREAM and RB cooperate to induce gene repression and cell-cycle arrest in response to p53 activation. *Nucleic Acids Res* **47**:9087–9103. doi:10.1093/nar/gkz635

Verfaillie A, Svetlichnyy D, Imrichova H, Davie K, Fiers M, Atak ZK, Hulselmans G, Christiaens V, Aerts S. 2016. Multiplex enhancer-reporter assays uncover unsophisticated TP53 enhancer logic. *Genome Res* **26**:882–895. doi:10.1101/gr.204149.116

Vyas P, Beno I, Xi Z, Stein Y, Golovenko D, Kessler N, Rotter V, Shakked Z, Haran TE. 2017. Diverse p53/DNA binding modes expand the repertoire of p53 response elements. *Proc Natl Acad Sci U S A* **114**:10624–10629. doi:10.1073/pnas.1618005114

Wang L, Wang S, Li W. 2012. RSeQC: quality control of RNA-seq experiments. *Bioinformatics* **28**:2184–2185. doi:10.1093/bioinformatics/bts356

Watanabe H, Ma Q, Peng S, Adelmant G, Swain D, Song W, Fox C, Francis JM, Pedamallu CS, DeLuca DS, Brooks AN, Wang S, Que J, Rustgi AK, Wong K, Ligon KL, Liu XS, Marto JA, Meyerson M, Bass AJ. 2014. SOX2 and p63 colocalize at genetic loci in squamous cell carcinomas. *J Clin Invest* **124**:1636–45. doi:10.1172/JCI71545

Westfall MD, Mays DJ, Sniezek JC, Pietenpol JA. 2003. The Np63 Phosphoprotein Binds the p21 and 14-3-3 Promoters In Vivo and Has Transcriptional Repressor Activity That Is Reduced by Hay-Wells Syndrome-Derived Mutations. *Mol Cell Biol* **23**:2264–2276. doi:10.1128/MCB.23.7.2264-2276.2003

Whitfield ML, George LK, Grant GD, Perou CM. 2006. Common markers of proliferation. *Nat Rev Cancer* **6**:99–106. doi:nrc1802 [pii]\r10.1038/nrc1802

Wu N, Rollin J, Masse I, Lamartine J, Gidrol X. 2012. p63 regulates human keratinocyte proliferation via MYC-regulated gene network and differentiation commitment through cell adhesion-related gene network. *J Biol Chem* **287**:5627–38. doi:10.1074/jbc.M111.328120

Yan W, Chen X. 2006. GPX2, a Direct Target of p63, Inhibits Oxidative Stress-induced Apoptosis in a p53-dependent Manner. *J Biol Chem* **281**:7856–7862. doi:10.1074/jbc.M512655200

Yang A, Kaghad M, Wang Y, Gillett E, Fleming MD, Dötsch V, Andrews NC, Caput D, McKeon F. 1998. P63, a P53 Homolog At 3Q27–29, Encodes Multiple Products With Transactivating, Death-Inducing, and Dominant-Negative Activities. *Mol Cell* **2**:305–16. doi:10.1016/S1097-2765(00)80275-0

Yang A, Schweitzer R, Sun D, Kaghad M, Walker N, Bronson RT, Tabin C, Sharpe A, Caput D, Crum C, McKeon F. 1999. p63 is essential for regenerative proliferation in limb, craniofacial and epithelial development. *Nature* **398**:714–8. doi:10.1038/19539

Yang A, Zhu Z, Kapranov P, McKeon F, Church GM, R T, Gingeras TR, Struhl K. 2006. Relationships between p63 Binding, DNA Sequence, Transcription Activity, and Biological Function in Human Cells. *Mol Cell* **24**:593–602. doi:10.1016/j.molcel.2006.10.018

Zarnegar BJ, Webster DE, Lopez-Pajares V, Vander Stoep Hunt B, Qu K, Yan KJ, Berk DR, Sen GL, Khavari PA. 2012. Genomic profiling of a human organotypic model of AEC syndrome reveals ZNF750 as an essential downstream target of mutant TP63. *Am J Hum Genet* **91**:435–43. doi:10.1016/j.ajhg.2012.07.007

Zhang Q, Huang D, Zhang Z, Feng Y, Fu M, Wei M, Zhou J, Huang Y, Liu S, Shi R. 2019. High expression of TMEM40 contributes to progressive features of tongue squamous cell carcinoma. *Oncol Rep* **41**:154–164. doi:10.3892/or.2018.6788

Zheng L, Zhao Z, Rong L, Xue L, Song Y. 2019. RASSF6-TRIM16 axis promotes cell proliferation, migration and invasion in esophageal squamous cell carcinoma. *J Genet Genomics*. doi:10.1016/j.jgg.2019.10.004

Zheng R, Wan C, Mei S, Qin Q, Wu Q, Sun H, Chen C-H, Brown M, Zhang X, Meyer CA, Liu XS. 2019. Cistrome Data Browser: expanded datasets and new tools for gene regulatory analysis. *Nucleic Acids Res* **47**:D729–D735. doi:10.1093/nar/gky1094

Figure 1

Meta-analysis of p63-dependent gene regulation. (A) Distribution of the number of genes found in each of the *p63 Expression Score* groups. Because *p63 Expression Score* group '13' and '-12' contained only 2 genes they were included in group '12' and '-11', respectively, for further analyses. **(B)** 16 datasets on p63-dependent gene expression from 11 studies. EE – exogenous p63 expression; sh KD – shRNA-mediated knockdown; si KD – siRNA-mediated knockdown; KO - sgRNA-mediated knockout **(C)** A heatmap displaying the regulation of 15 genes with positive and 15 genes with negative *p63 Expression Scores*. *GAPDH* and *GAPDHS* represent negative controls.

Figure 2

Gene sets enriched among genes commonly regulated by p63. Enrichment of **(A, B, C, E)** MSigDB gene sets or **(D)** genes up- and down-regulated across squamous cell cancers (SCC) (Campbell et al., 2018) among genes ranked by the *p63 Expression Score*.

Figure 3

Transcription factors in the p63 GRN. (A) Significant (adj.p-value ≤ 0.05) enrichment of TF binding at genes with a *p63 Expression Score* ≥ 8 (green) or ≤ -8 (red) as identified by Enrichr (Kuleshov et al., 2016). **(B)** Enrichment of MSigDB gene sets among genes ranked by the *p63 Expression Score*. Scatter plots displays the $\log_2$(fold-change) of previously

collected high confidence DREAM target genes (Fischer et al., 2016a) **(C)** across the 16 p63-dependent gene expression profiling datasets and **(D)** MCF10A cells treated with DMSO or Nutlin in addition to shControl and shp63 (Karsli Uzunbas et al., 2019). *CDKN1A* levels serve as control. The black line indicates the median.

Figure 4

p63 and p53 regulate largely distinct target gene sets. (A) The *p63 Expression Score* compared to the previously published *p53 Expression Score* that was generated using the same meta-analysis approach (Fischer et al., 2016a) for all 16,198 genes for which both scores were available. **(B)** The scatter plot displays the $\log_2$(fold-change) of previously collected high confidence direct p53 target genes (Fischer, 2017) across the 16 p63-dependent gene expression profiling datasets. The black line indicates the median. The data indicates a large degree of independence of p53 targets from p63-dependent expression.

Figure 5

The p63 and p53 DNA binding landscape. (A and B) The number of p63 and p53 binding peaks sorted by the number of datasets that commonly identified/support the peak. **(C)** The number of p53 and p63 peaks identified in the 28 p53 and 20 p63 ChIP-seq datasets, respectively. **(D)** The relative number of 'known' p53 and p63 motifs found by HOMER v4.10 (Heinz et al., 2010) under p53 and p63 peaks, respectively, with increasing dataset support. **(E)** Schematic of 'p53', 'p63' and 'p53+p63' peak selection for further analyses. **(F)** *De novo* motif search results from HOMER v4.10 (Heinz et al., 2010) for the 'p53+p63', 'p53', and 'p63' peak sets. The first round of motif search identified the 'primary' motif in each peak set. Using an iterative approach, all peaks that contained the 'primary' motif were removed and the *de novo* motif search was repeated. This iterative approach was followed until no more p53/p63-like motif was identified.

Figure 6

The DNA binding landscape of p53. DNA sites occupied by p53 in at least 5 datasets were searched iterative with the motifs identified by our iterative *de novo* search (Figure 5F). We searched first for the primary 'p53+p63' motif and among all remaining sites for the primary 'p53' motif. All other 'p53+p63' and 'p53' motifs were searched subsequently.

Figure 7

The DNA binding landscape of p63. DNA sites occupied by p63 in at least 5 datasets were searched iterative with the motifs identified by our iterative *de novo* search (Figure 5F). We searched first for the primary 'p53+p63' motif and among all remaining sites

for the primary ‘p63’ motif. All other ‘p53+p63’ and ‘p63’ motifs were searched subsequently (Supplementary File 3).

Figure 8

p63/SCC 28-gene set correlates with poorer survival in HNSC. Kaplan-Meier plots of TCGA HNSC patient survival data. **(A**) Patients were subdivided in four equally sized subgroups based on expression levels of the 28-gene set. The results suggest a poorer survival of patients with an up-regulated expression of the set genes. **(B)** To corroborate this finding patients of the subgroups low-med, med-high, and high from (A) were joined to form a new high group. Boxplot in bins of 10 of *TP63* FPKM expression values in TCGA HNCS patient sample data compared to **(C)** FPKM values of a meta-gene comprising the 28-gene set and **(D)** ssGSEA scores of the 28-gene set. X-axis is right-censored at 100 to better visualize the effect. The full graph is displayed in Figure 8-figure supplement 1.

Figure 5-figure supplement 1

(A and B) Correlation between dataset support for p53 and p63 binding. **(C to F)** Correlation between HOMER motif score for primary and secondary ‘p53+p63’ motifs and dataset support for **(C and D)** p53 binding or **(E and F)** p63 binding.

Figure 5-figure supplement 2

Correlation between HOMER motif score for primary, secondary and tertiary **(A to C)** ‘p53’ motifs or **(D to F)** ‘p63’ motifs and dataset support for **(A to C)** p53 binding or **(D to F)** p63 binding.

Figure 5-figure supplement 3

Top motifs co-enriched with primary ‘p53+p63’, ‘p53’, and ‘p63’ motifs at the respective DNA sites.

Figure 5-figure supplement 4

Top 20 TFs with ChIP-seq peak sets similar to **(A)** the common p53+p63 sites, **(B)** the unique p53 sites, and **(C)** the unique p63 sites (Figure 5E) as identified using CistromeDB toolkit. Of note, some TP53 ChIP-seq datasets are wrongly labeled “T” in the database.

Figure 7-figure supplement 1

Complement to Table 1. Genes identified as significantly up- or down-regulated in at least the half of all datasets (|*p63 Expression Score*| ≥ 8) that are linked to p63 binding sites supported by at least half of all datasets (≥ 10) through binding within 5 kb from their TSS or

through double-elite enhancer:gene associations (Fishilevich et al., 2017). Using these thresholds we identified 138 and 42 high-probability candidates as directly up- and down-regulated by p63, respectively. Gene names marked in red are also up- or down-regulated across SCCs (Campbell et al., 2018).

Figure 8-figure supplement 1

Boxplot in bins of 10 of *TP63* FPKM expression values in TCGA HNCS patient sample data compared to **(A)** FPKM values of a meta-gene comprising the 28-gene set and **(B)** ssGSEA scores of the 28-gene set. Complementary to Figure 8C and D.

Supplementary File 1

Detailed information on publicly available p63-dependent gene expression profiling and p63 ChIP-seq datasets that were integrated in this study.

Supplementary File 2

Meta-analysis from 16 p63-dependent gene expression information datasets (listed in Suppelemtary File 1) to generate the *p63 Expression Score* for 19,156 human genes.

Supplementary File 3

p63 and p53 binding sites identified in at least 5 out of 20 and 28 ChIP-seq datasets, respectively. Binding sites are listed with their ChIP-seq dataset support and highest scoring p63 response elements (p63REs) or p53REs. Genes associated with p63 binding sites through proximal TSS binding or enhancers are listed.

Riege *et al.*, Figure 1

A

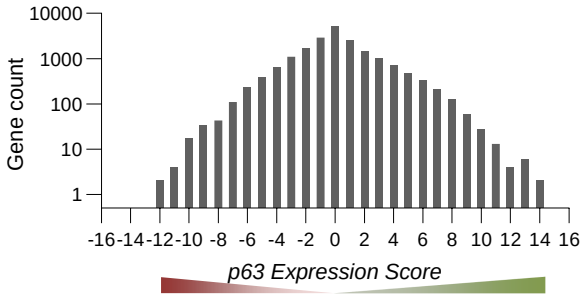

B

Reference	p63 status	cells	platform	# genes covered	# genes sig. regulated up	# genes sig. regulated down
Carroll 2006	EE	MCF10A	microarray	11,358	1,291	1,716
	sh KD	MCF10A		11,358	1,893	2,047
Zarnegar 2012	EE	KC	microarray	17,883	4,119	4,119
	si KD	KC		17,883	1,951	3,396
Wu 2012	si KD	HaCaT	microarray	11,580	1,046	873
Gallant-Behm 2012	sh KD	H226	microarray	16,470	2,264	1,890
Watanabe 2014	sh KD	KYSE70	RNA-seq	12,866	354	580
Bao 2015	sh KD	KC	RNA-seq	17,219	4,475	4,620
Saladi 2017	sh KD	HaCaT	microarray	16,403	4,386	2,618
	sh KD	FaDu		16,403	1,512	1,057
Abraham 2018	sh KD	H226	RNA-seq	15,984	4,053	4,550
Somerville 2018	sh KD / KO	BxPC3	RNA-seq	16,153	871	1,373
	EE	SUIT2		12,756	1,317	927
Uzunbas 2019	sh KD	MCF10A	RNA-seq	12,968	2,105	1,568
	sh KD +Nutlin	MCF10A		13,180	2,940	2,198
Lin-Shiao 2019	EE	BJ	RNA-seq	16,464	2,530	1,544

C

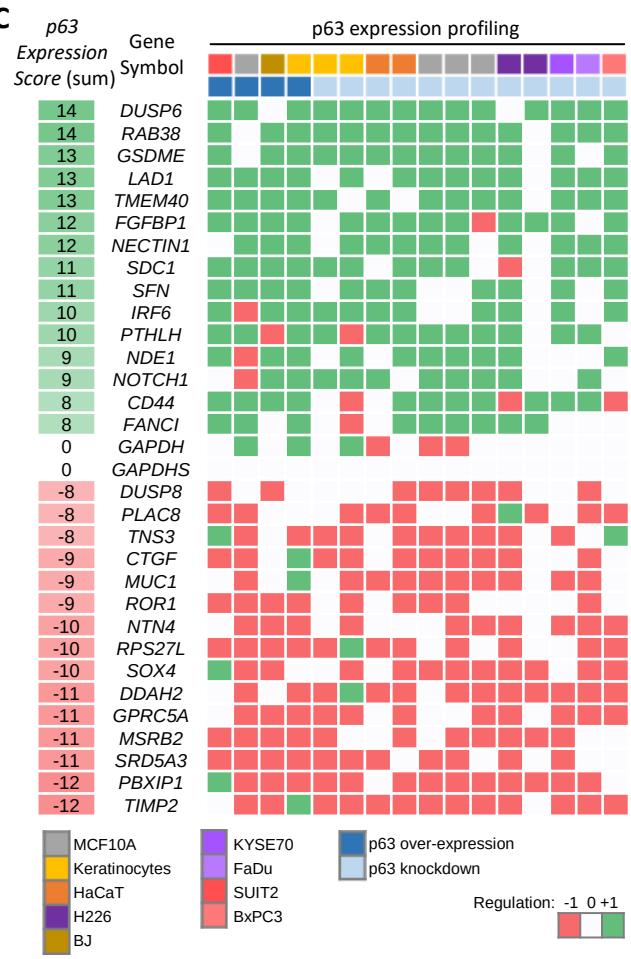

Riege *et al.*, Figure 2

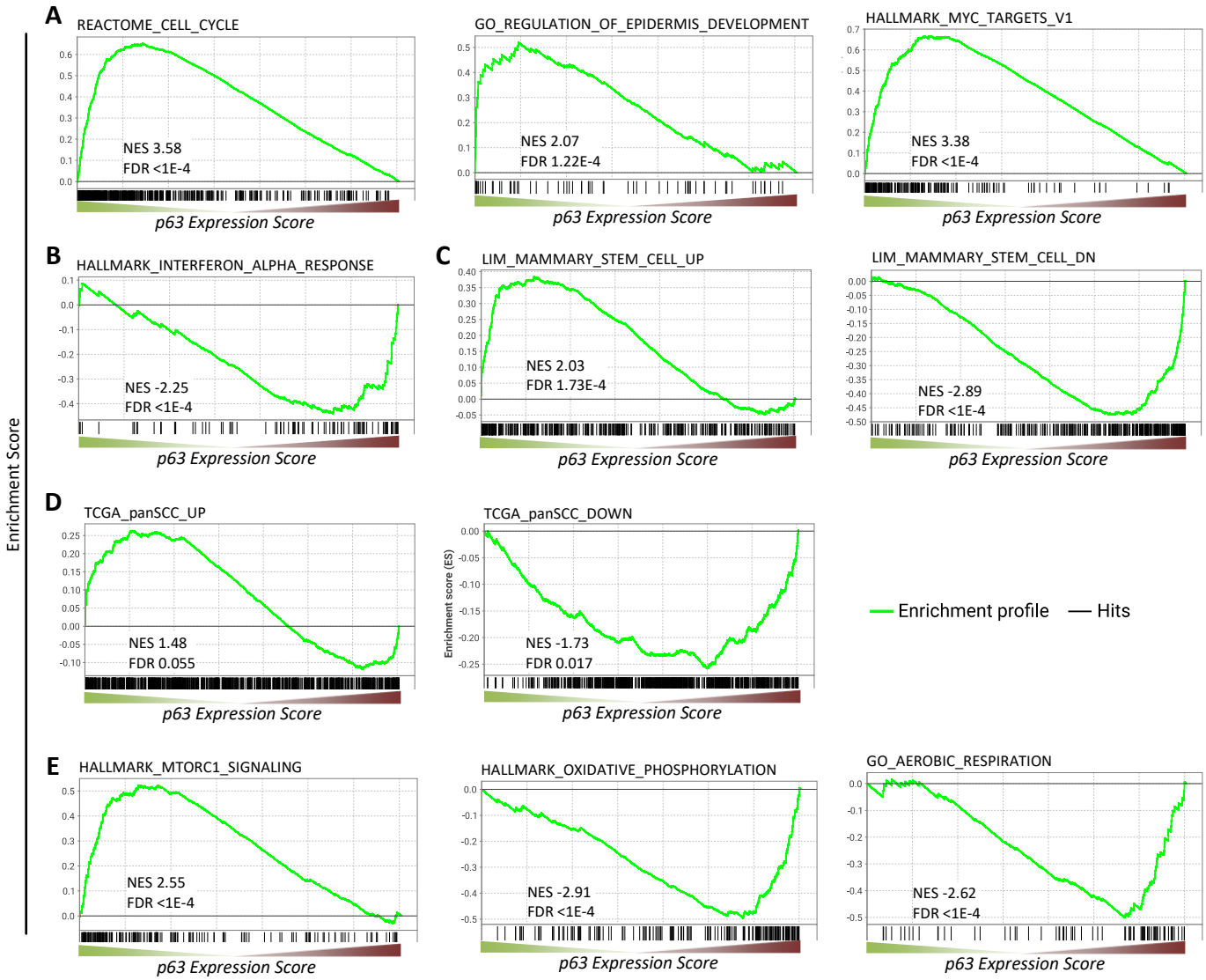

Riege *et al.*, Figure 3

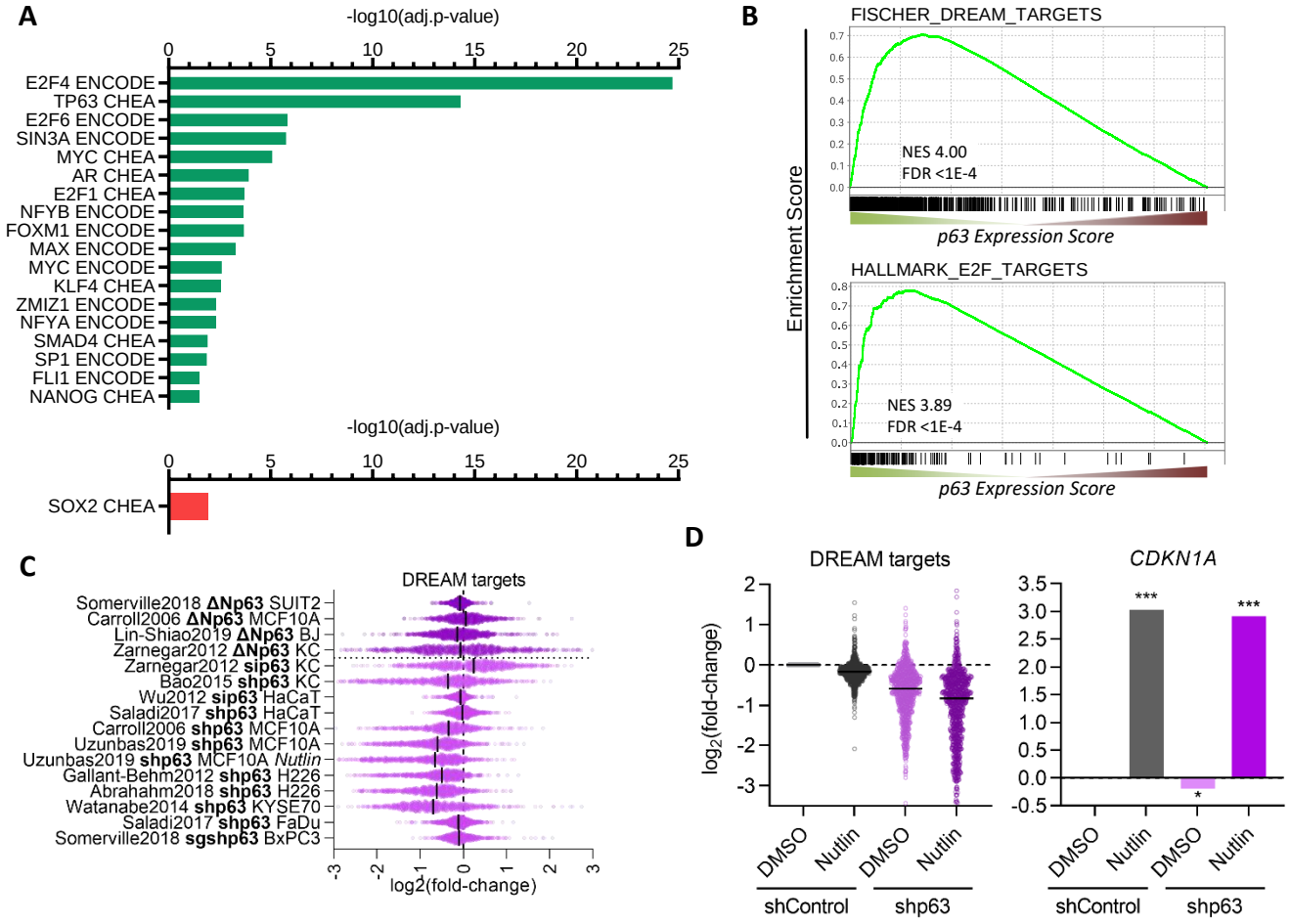

Riege *et al.*, Figure 4

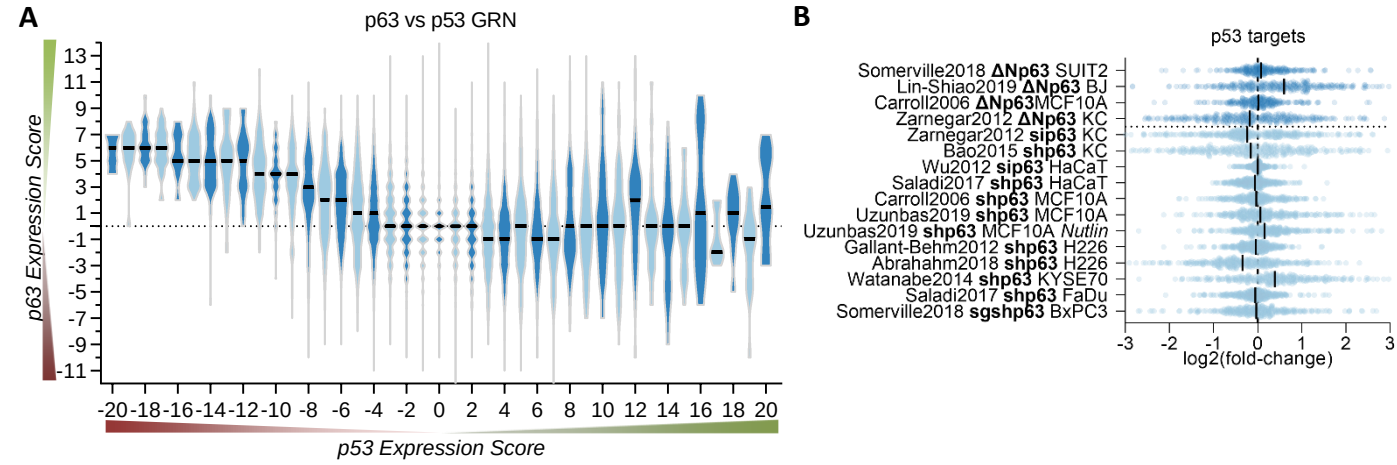

Riege *et al.*, Figure 5

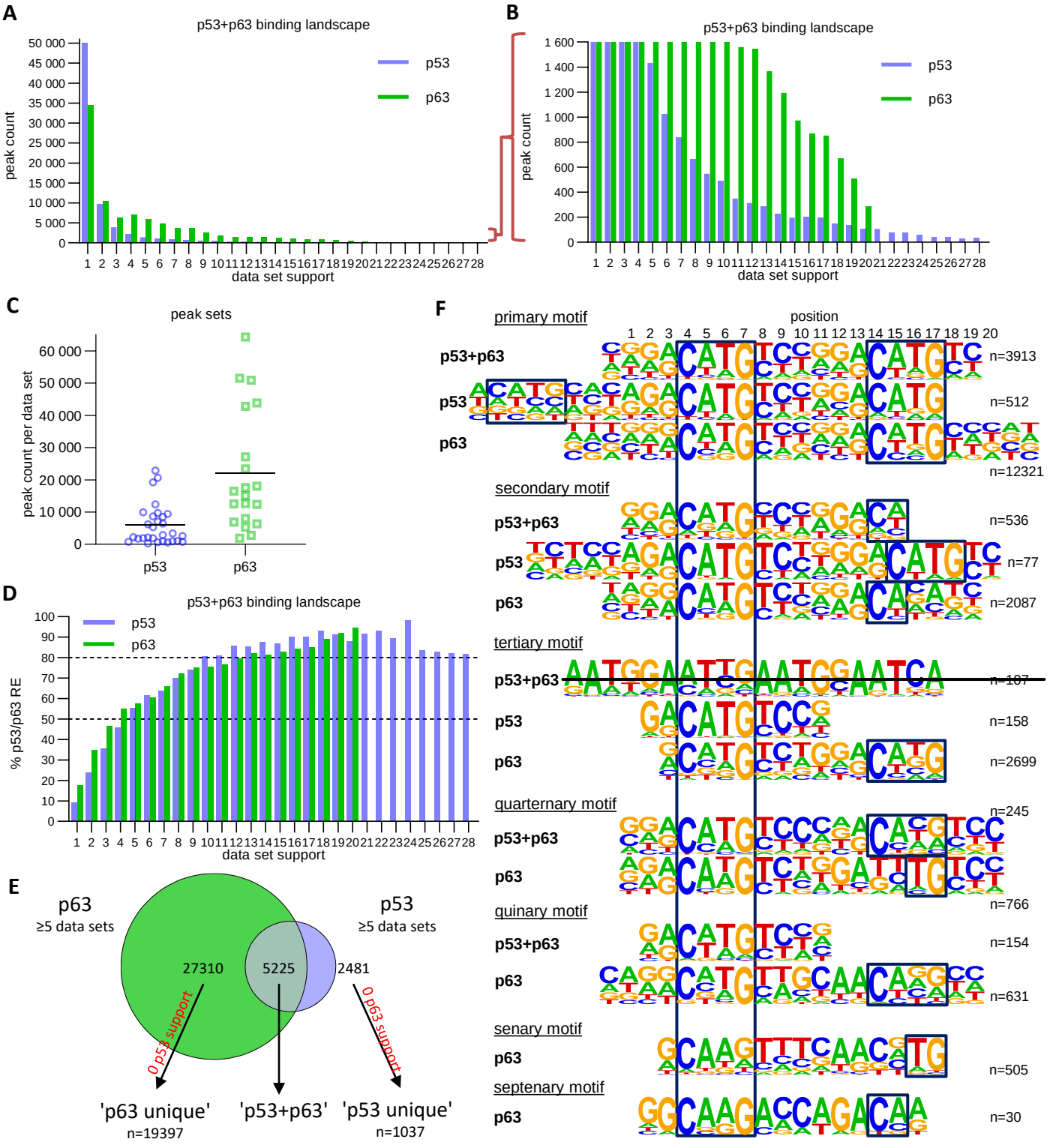

Riege *et al.*, Figure 5 – figure supplement 1

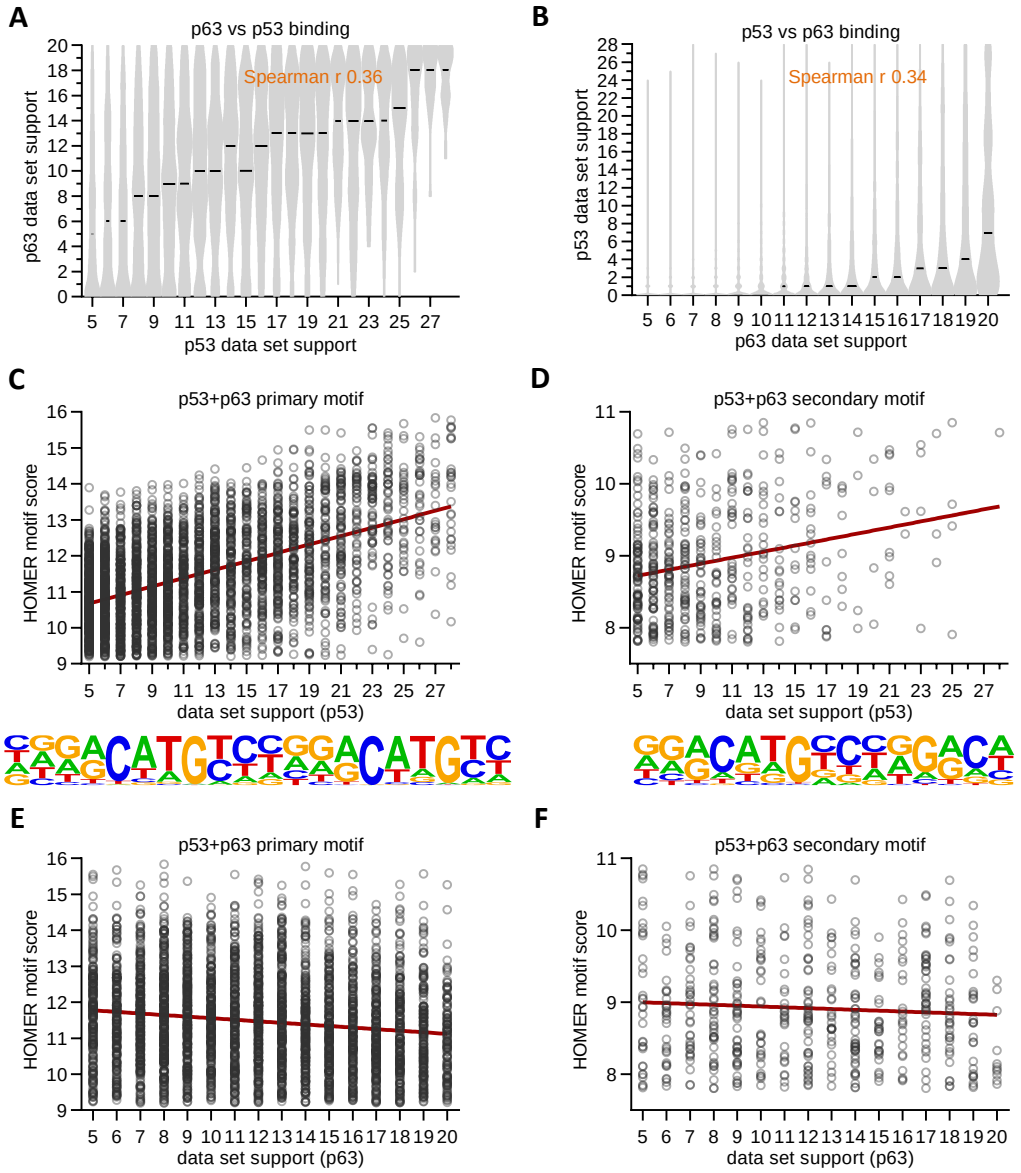

(A and B) Correlation between data set support for p53 and p63 binding. (C to F) Correlation between HOMER motif score for primary and secondary 'p53+p63' motifs and data set support for **(C and D)** p53 binding or **(E and F)** p63 binding

Riege *et al*., Figure 5 – figure supplement 2

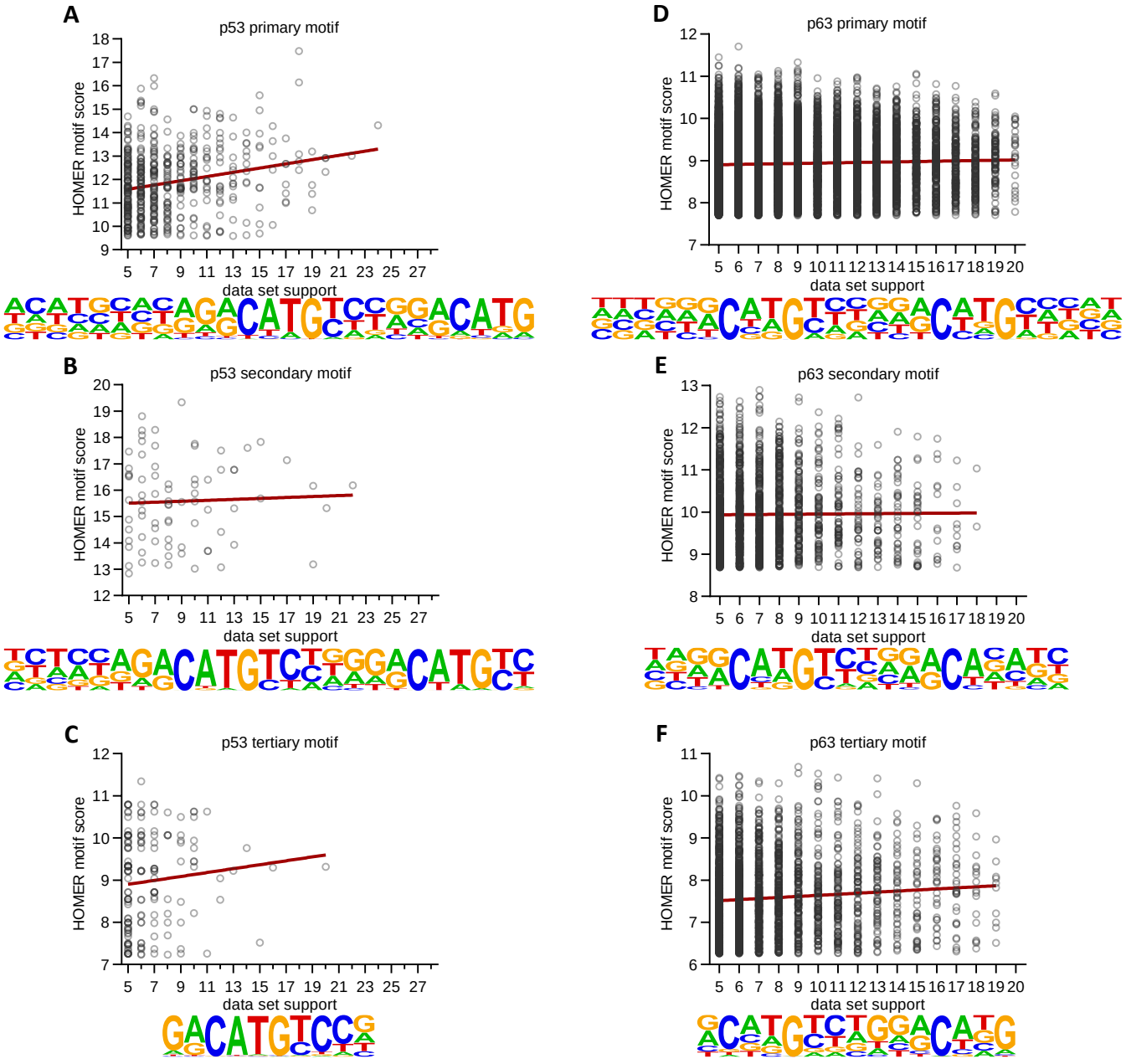

Correlation between HOMER motif score for primary, secondary and tertiary **(A to C)** 'p53' motifs or **(D to F)** 'p63' motifs and data set support for **(A to C)** p53 binding or **(D to F)** p63 binding.

Riege *et al.*, Figure 5 – figure supplement 3

Top3 *de novo* motifs identified

p53+p63 common sites

Motif	p-value	% targets	% background	similarity
	1E-6729	74.84%	0.90%	p53
	1E-382	3.04%	0.01%	unknown
	1E-256	1.95%	0.00%	GATA

p53 unique sites

Motif	p-value	% targets	% background	similarity
	1E-662	52.63%	1.38%	p53
	1E-163	6.08%	0.01%	unknown
	1E-131	5.56%	0.01%	GATA

p63 unique sites

Motif	p-value	% targets	% background	similarity
	1E-11463	65.20%	4.46%	p63
	1E-761	23.99%	9.32%	AP-1 (bZIP)
	1E-525	36.63%	21.03%	bHLH

Top motifs co-enriched with primary ‘p53+p63’, ‘p53’, and ‘p63’ motifs at the respective DNA sites.

Riege *et al.*, Figure 5 – figure supplement 4

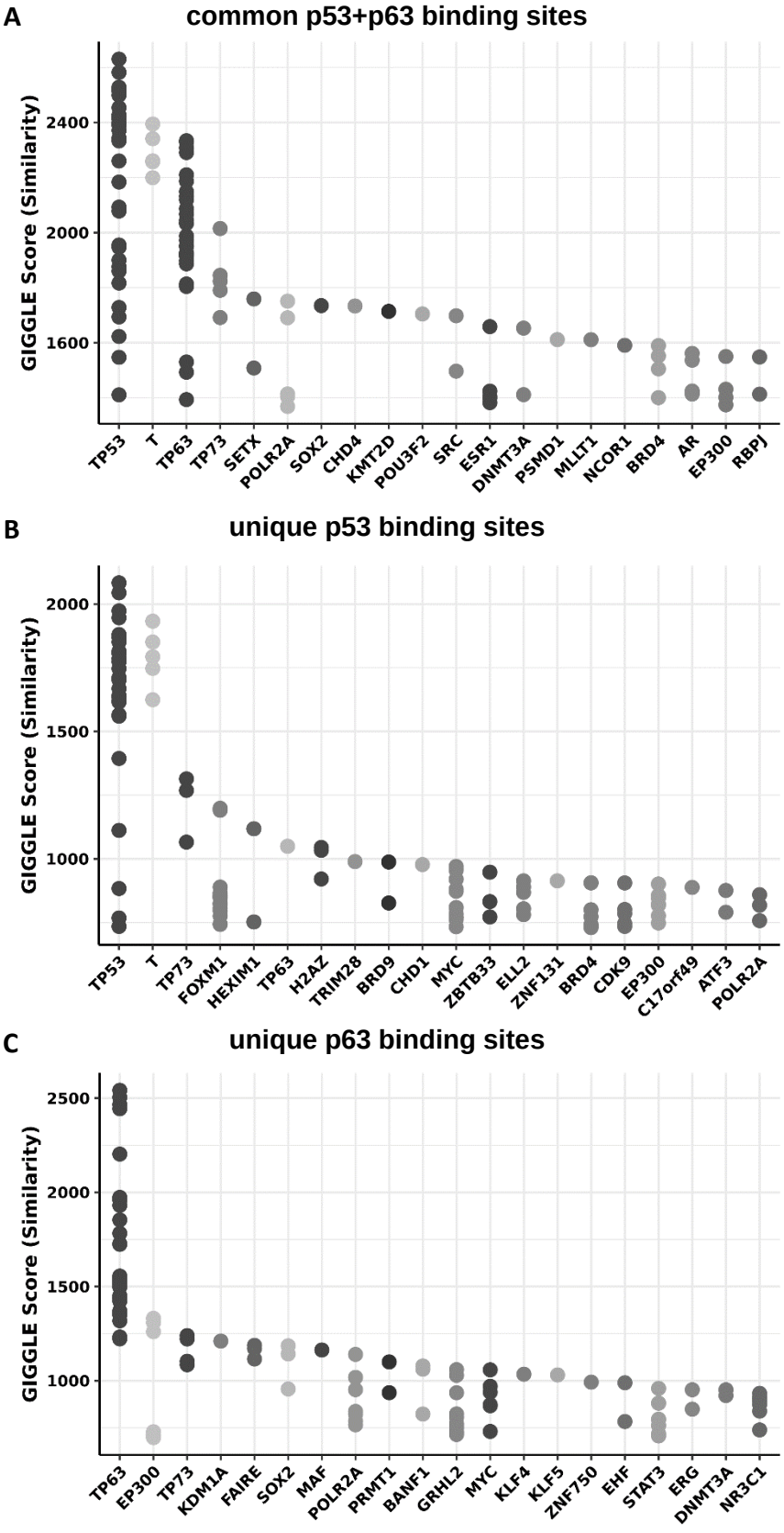

Top 20 TFs that possess ChIP-seq peaksets similar to **(A)** the common p53+p63 sites, **(B)** the unique p53 sites, and **(C)** the unique p63 sites (Figure 5E) as identified using CistromeDB toolkit. Of note, some TP53 ChIP-seq data sets are wrongly labeled “T” in the database.

Riege *et al.*, Figure 6

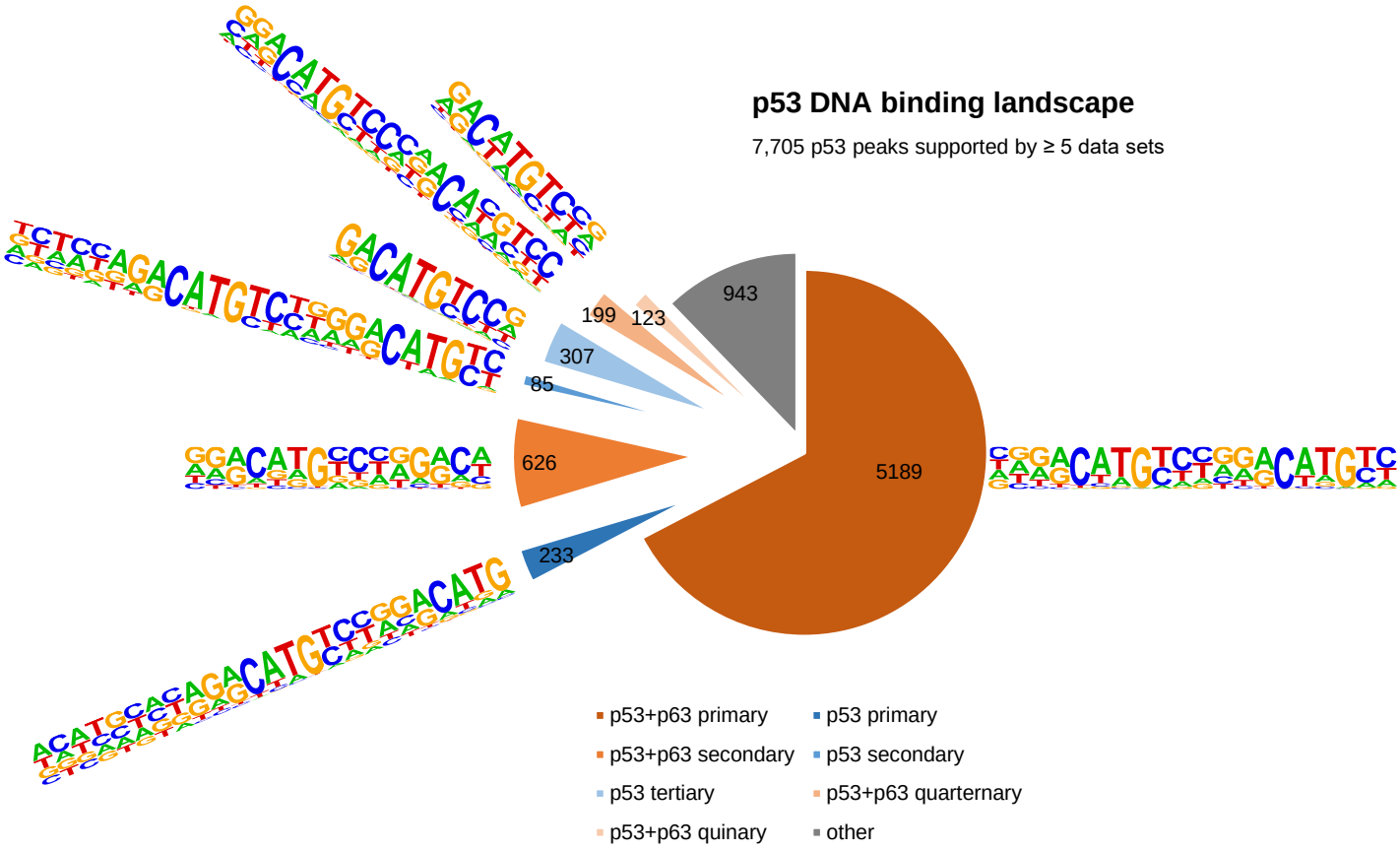

Riege *et al.*, Figure 7

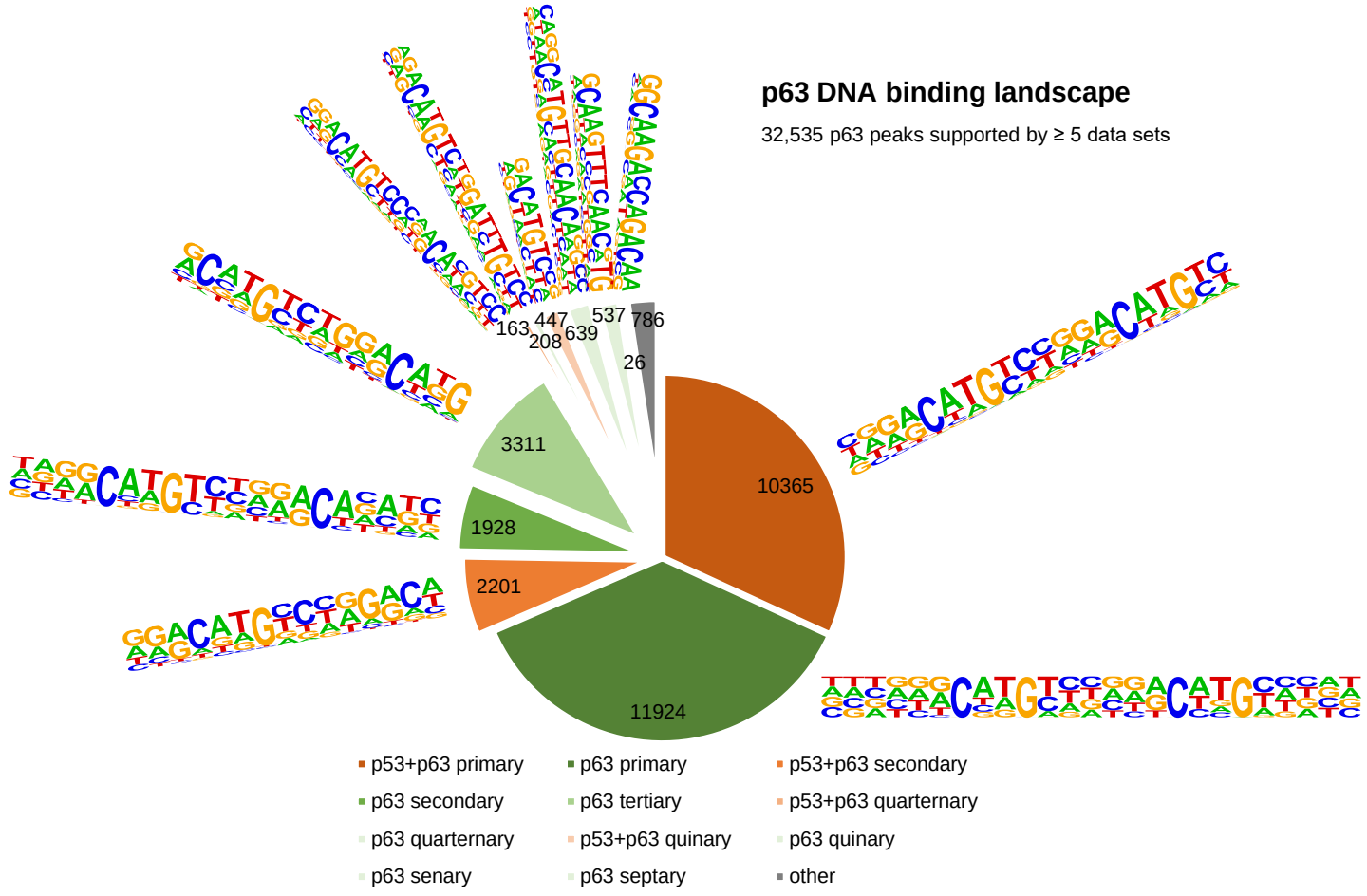

Riege *et al.*, Figure 7 – figure supplement 1

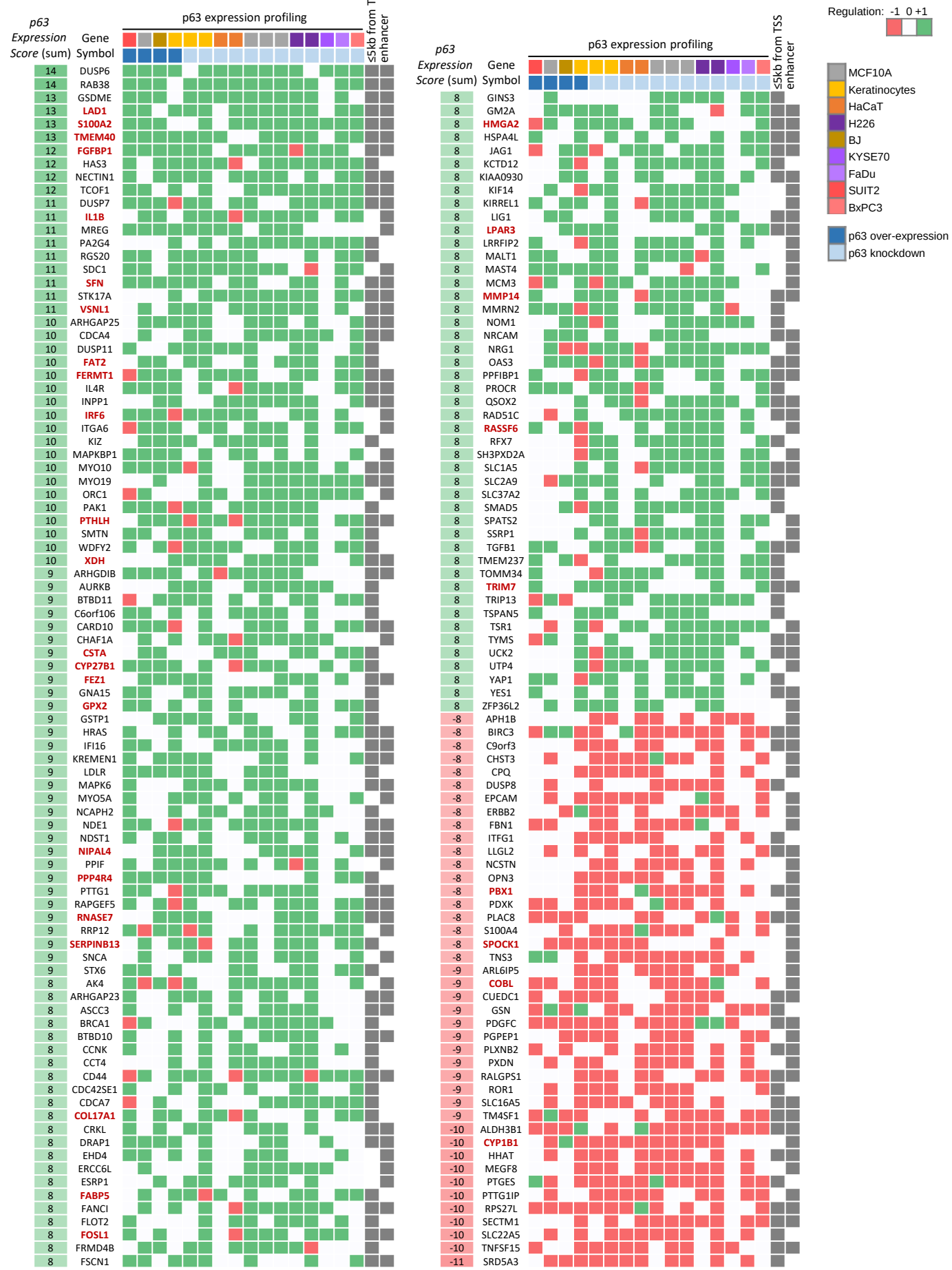

Figure 7 – figure supplement 1

Complement to Table 1. Genes identified as significantly up- or down-regulated in at least the half of all datasets (|*p63 Expression Score*| ≥ 8) that are linked to p63 binding sites supported by at least half of all datasets (≥ 10) through binding within 5 kb from their TSS or through double-elite enhancer:gene associations (Fishilevich et al., 2017). Using these thresholds we identified 138 and 42 high-probability candidates as directly up- and down-regulated by p63, respectively. Gene names marked in red are also up- or down-regulated across SCCs (Campbell et al., 2018).

Riege *et al.*, Figure 8

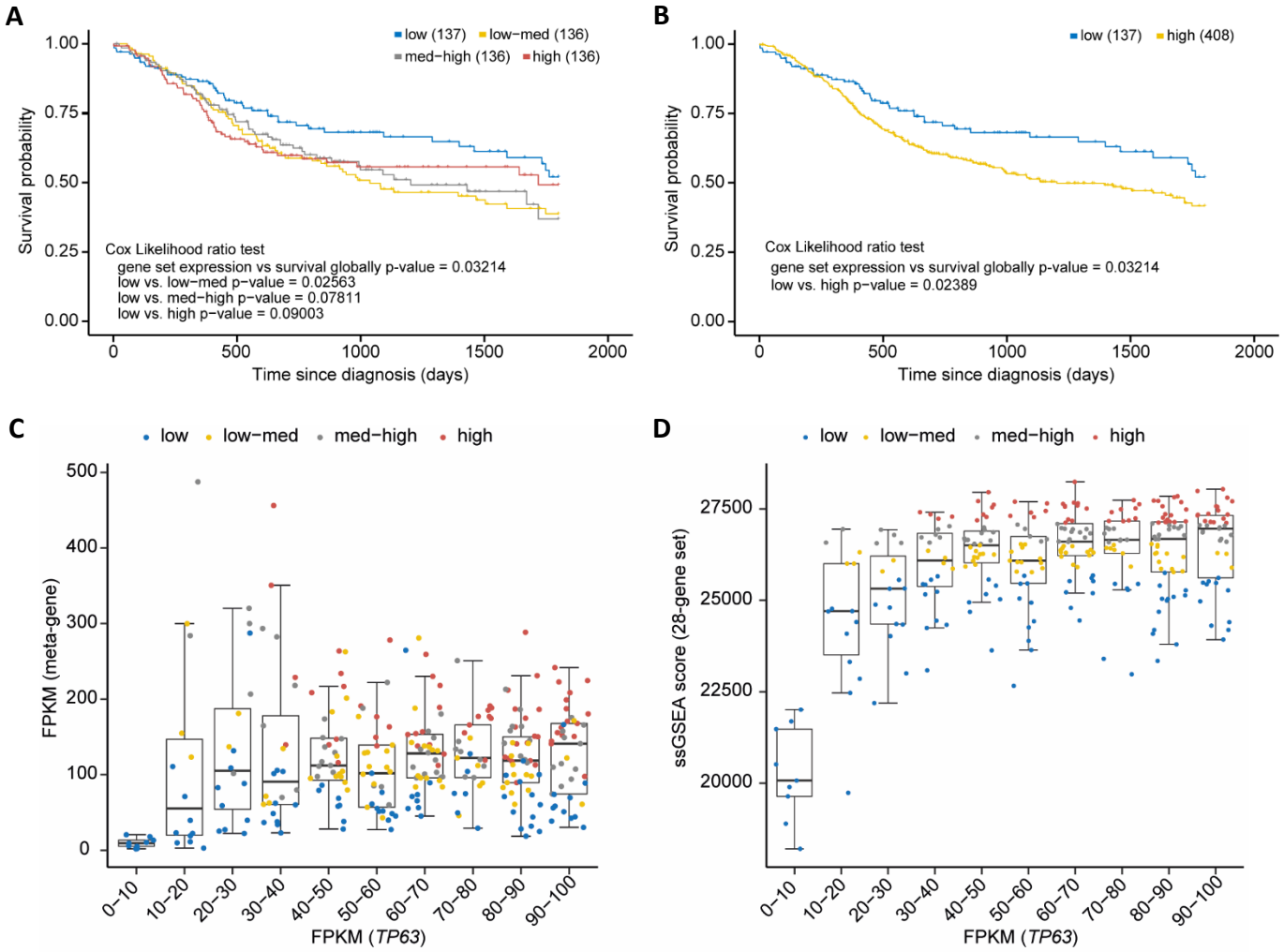

Riege *et al.*, Figure 8 – figure supplement 1

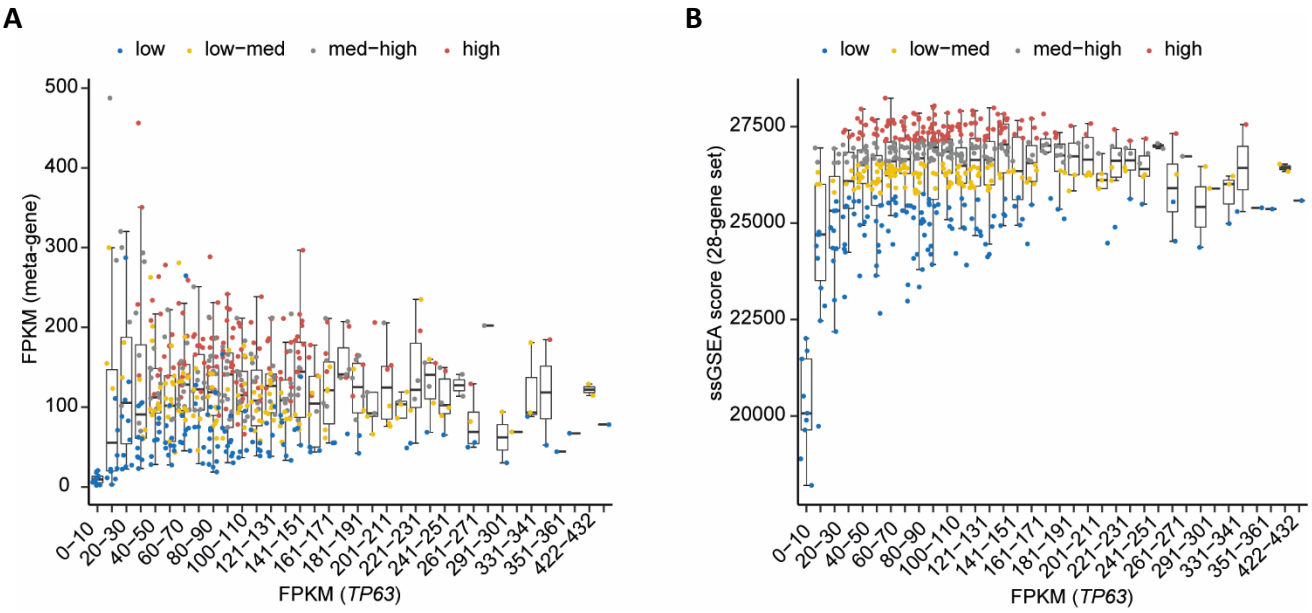

Boxplot in bins of 10 of *TP63* FPKM expression values in TCGA HNCS patient sample data compared to **(A)** FPKM values of a meta-gene comprising the 28-gene set and **(B)** ssGSEA scores of the 28-gene set. Complementary to Figure 8C and D.